microRNA-122 Abundance in Hepatocellular Carcinoma and Non-Tumor Liver Tissue from Japanese Patients with Persistent HCV versus HBV Infection

Carolyn Spaniel[1,2], Masao Honda[3], Sara R. Selitsky[1,4], Daisuke Yamane[1], Tetsuro Shimakami[3], Shuichi Kaneko[3], Robert E. Lanford[5], Stanley M. Lemon[1*]

1 Departments of Medicine and Microbiology & Immunology and the Lineberger Comprehensive Cancer Center, the University of North Carolina at Chapel Hill, Chapel Hill, North Carolina, United States of America, **2** Department of Microbiology and Immunology, University of Texas Medical Branch, Galveston, Texas, United States of America, **3** Department of Gastroenterology, Kanazawa University Graduate School of Medicine, Takara-Machi, Kanazawa, Japan, **4** Department of Genetics, the University of North Carolina at Chapel Hill, Chapel Hill, North Carolina, United States of America, **5** Department of Virology and Immunology, Texas Biomedical Research Institute, San Antonio, Texas, United States of America

Abstract

Mechanisms of hepatic carcinogenesis in chronic hepatitis B and hepatitis C are incompletely defined but often assumed to be similar and related to immune-mediated inflammation. Despite this, several studies hint at differences in expression of miR-122, a liver-specific microRNA with tumor suppressor properties, in hepatocellular carcinoma (HCC) associated with hepatitis B virus (HBV) versus hepatitis C virus (HCV) infection. Differences in the expression of miR-122 in these cancers would be of interest, as miR-122 is an essential host factor for HCV but not HBV replication. To determine whether the abundance of miR-122 in cancer tissue is influenced by the nature of the underlying virus infection, we measured miR-122 by qRT-PCR in paired tumor and non-tumor tissues from cohorts of HBV- and HCV-infected Japanese patients. miR-122 abundance was significantly reduced from normal in HBV-associated HCC, but not in liver cancer associated with HCV infection. This difference was independent of the degree of differentiation of the liver cancer. Surprisingly, we also found significant differences in miR-122 expression in non-tumor tissue, with miR-122 abundance reduced from normal in HCV- but not HBV-infected liver. Similar differences were observed in HCV- vs. HBV-infected chimpanzees. Among HCV-infected Japanese subjects, reductions in miR-122 abundance in non-tumor tissue were associated with a single nucleotide polymorphism near the IL28B gene that predicts poor response to interferon-based therapy (TG vs. TT genotype at rs8099917), and correlated negatively with the abundance of multiple interferon-stimulated gene transcripts. Reduced levels of miR-122 in chronic hepatitis C thus appear to be associated with endogenous interferon responses to the virus, while differences in miR-122 expression in HCV- versus HBV-associated HCC likely reflect virus-specific mechanisms contributing to carcinogenesis. The continued expression of miR-122 in HCV-associated HCC may signify an important role for HCV replication late in the progression to malignancy.

Citation: Spaniel C, Honda M, Selitsky SR, Yamane D, Shimakami T, et al. (2013) microRNA-122 Abundance in Hepatocellular Carcinoma and Non-Tumor Liver Tissue from Japanese Patients with Persistent HCV versus HBV Infection. PLoS ONE 8(10): e76867. doi:10.1371/journal.pone.0076867

Editor: Birke Bartosch, Inserm, U1052, UMR 5286, France

Received May 19, 2013; **Accepted** August 29, 2013; **Published** October 9, 2013

Copyright: © 2013 Spaniel et al. This is an open-access article distributed under the terms of the Creative Commons Attribution License, which permits unrestricted use, distribution, and reproduction in any medium, provided the original author and source are credited.

Funding: This work was supported in part by National Institutes of Health grants R01-AI095690 and R01-CA164029 and the University Cancer Research Fund. The funders had no role in study design, data collection and analysis, decision to publish, or preparation of the manuscript.

Competing interests: The authors have declared that no competing interests exist.

* E-mail: smlemon@med.unc.edu

Introduction

Globally, liver cancer is the fifth and seventh most common malignancy in men and women, respectively, and the third most deadly [1]. Most (85-95%) of these cancers are hepatocellular carcinoma (HCC) [2], and many are associated with persistent intrahepatic infections with hepatitis C virus (HCV) or hepatitis B virus (HBV) [2,3]. Although the total cancer death rate decreased within the United States by over 1.5% between 2001-2007, deaths due to liver cancer increased by 50% among males and by 29% in females [4]. These changes in the incidence of HCC are largely due to increases in HCV-associated malignancy. Similarly, while HBV infection historically has been the major risk factor underlying development of HCC in Asia, in Japan it has been supplanted in recent decades by HCV infection [5].

The exact mechanisms underlying HCV- and HBV-associated malignancy are unknown [6,7]. Chronic infections with either virus may result in cirrhosis, which alone is a major risk factor for liver cancer [2]. However, there may also be

virus-specific mechanisms at work. While immune-mediated mechanisms are both necessary and sufficient for the development of HBV-related cancer in murine models, liver cancer arises in the absence of inflammation in HCV-transgenic mice [8,9]. Moreover, some HCV proteins may interact with host tumor suppressors and possibly impair cellular responses to DNA damage [10]. If virus-specific mechanisms of oncogenesis are important in the development of HCC, it is reasonable to anticipate that the pathways leading to HCV- and HBV-associated cancer might differ, possibly leaving distinguishing genetic or epigenetic marks in the tumors that arise. If so, understanding these differences would be important for biomarker discovery, and potentially design of preventative and therapeutic interventions.

Here, we describe a study that was aimed at determining whether the abundance of microRNA-122 (miR-122) is different in liver cancer arising in patients with chronic HCV infection compared to cancers arising in the context of chronic HBV infection. Mature microRNAs (miRNAs) are 20-23 nucleotides in length and encoded either by microRNA genes or from within conventional protein-coding genes. They act generally by binding to specific sites within the 3' untranslated region (3' UTR) of cellular mRNAs, to which they recruit RNA-induced silencing complexes (RISC) that repress translation and destabilize the mRNA [11–13]. miR-122 is a liver-specific miRNA that accounts for the majority of miRNAs in hepatocytes [14]. It regulates a large number of genes within the liver [15], and has several tumor suppressor-like properties [16,17]. Importantly, miR-122 is a crucial host factor for HCV replication, binding to the 5' untranslated RNA segment of the viral genome, physically stabilizing it, and promoting viral protein expression [18–20].

Because of its liver-specific nature and tumor suppressor-like qualities [16,17], it is of interest to know whether miR-122 expression is altered in liver cancers. Prior studies investigating miR-122 expression in liver cancers have produced conflicting results, particularly as related to the underlying viral causes of cancer. Two early studies suggest that miR-122 abundance is generally reduced in HCC [21,22]. However, Hou et al. [23] reported that miR-122 expression was maintained in both HBV- and HCV-associated cancer, while Varnholt et al. [24] reported that miR-122 levels were increased significantly in HCV-associated cancers when compared to non-cancerous tissue. Coulouarn et al. [25] reported higher miR-122 expression levels in HCV- versus HBV-associated cancers. To some extent, these conflicting results may reflect different patient populations, or possibly methodologic differences, not only in the measurement of miR-122 abundance but also in how miR-122 abundance was compared across tissue samples.

In an effort to resolve this controversy, we conducted a comprehensive analysis of miR-122 expression in liver cancers arising in a genetically homogenous group of Japanese patients. Using a highly accurate, miR-122-specific quantitative reverse-transcription, polymerase chain reaction (qRT-PCR) assay, and paying particular attention to how miR-122 measurements are compared between tissue samples, we show that miR-122 expression is significantly reduced in HBV-associated HCC but not in most HCV-associated cancers. We also demonstrate that miR-122 abundance is reduced in non-tumor HCV-infected liver in association with increased expression of interferon (IFN)-stimulated genes (ISGs).

Materials and Methods

Ethics statement

Liver tissue was obtained from Japanese patients undergoing surgical resection of liver cancer (primary or metastatic) at the Liver Center of Kanazawa University Hospital (Kanazawa, Japan). All subjects provided written informed consent for participation in the study, and tissue acquisition procedures were approved by the ethics committee of Kanazawa University under a protocol entitled "Gene expression analysis of peripheral blood cells and liver in patients with liver and gastrointestinal cancers". Archived liver tissue and serum samples were collected prior to December 15, 2011 from chimpanzees housed and cared for at the Southwest National Primate Research Center (SNPRC) of the Texas Biomedical Research Institute in accordance with the Guide for the Care and Use of Laboratory Animals. All protocols were approved by the Institutional Animal Care and Use Committee. SNPRC is accredited by the Association for Assessment and Accreditation of Laboratory Animal Care (AAALAC) International and operates in accordance with the NIH and U.S. Department of Agriculture guidelines and the Animal Welfare Act.

Human subjects and tissue samples

Paired samples of HCC and non-tumor liver tissue were obtained from Japanese patients undergoing surgical resection of HCC at the Liver Center of Kanazawa University Hospital (Kanazawa, Japan). Non-infected 'normal' liver tissue was similarly collected from patients undergoing resection of metastases of non-hepatic primary cancers. Patients were categorized as HCV-infected by the presence of HCV RNA (COBAS Ampli-Prep/COBAS TaqMan System) and absence of hepatitis B surface antigen (HBsAg) in serum or plasma at the time of surgery, while HBV infection was defined by the presence of HBsAg and absence of anti-HCV antibodies. HCC was categorized according to the degree of cellular differentiation, while fibrosis and inflammation in non-tumor tissue from HBV- and HCV-infected patients were compared after scoring each [26,27]. The IL28B genotype of study subjects with HCV infection was defined at the rs8099917 locus as described previously [28].

Chimpanzee care and sample collection

We studied archived liver tissue and serum samples collected prior to December 15, 2011 from chimpanzees housed and cared for at the Southwest National Primate Research Center (SNPRC) of the Texas Biomedical Research Institute. At the time samples were obtained, animals considered to be non-infected ('normal') were negative for HBV and HCV markers; HBV infection was defined as the presence of serum HBsAg, and HCV infection by the presence of HCV RNA detectable in sera by RT-PCR.

Small RNA quantitation in human samples

Human tissue samples were stored in liquid nitrogen until processed for RNA extraction. Approximately 1 mg of tissue was ground using a tissue homogenizer and total RNA isolated using the mirVana miRNA isolation kit (Ambion). Liver RNA samples were subsequently stored at -80°C or on dry ice during shipment. The quality of the isolated RNA (RIN score) was assessed using an Agilent 2100 Bioanalyzer (Agilent RNA 6000 Nano Kit, Agilent Technologies) [29]. Quantification of miR-122, miR-191, Let-7a, miR-24, and the small nuclear RNA (snRNA) U6 was carried out by quantitative reverse-transcription, polymerase chain reaction (qRT-PCR) in a two-step process. RNA (12.5 ng) was reversed transcribed in a 10 µl reaction mix using reagents provided with the Universal cDNA Synthesis kit (Exiqon) and the manufacturer's recommended procedure. Quantitative PCR was carried out subsequently with the SYBR Green Master Mix Kit (Exiqon), mixed locked-nucleic acid primer sets specific for each miRNA or snRNA (Exiqon), and the CFX96 PCR System (Bio-Rad). Results are presented as relative copy number normalized to total RNA. Alternatively, absolute miR-122 copy numbers were estimated using serial dilutions of single-stranded synthetic miR-122 (Dharmacon) as a standard.

miR-122 and HCV RNA quantitation in chimpanzee samples

Total RNA was extracted from serum and liver using RNA Bee (Leedo Medical Labs, Houston, TX), chloroform extraction and isopropanol precipitation. Detection of miR-122 was performed using primers and probes for miR-122 included in the ABI TaqMan assay (Cat No. 4373151) and the ABI TaqMan microRNA Reverse Transcription Kit (Cat No. 4366596). The RT reaction was performed with 5 ng of total cell RNA, and the PCR amplification was performed with one-tenth of the resulting cDNA. The RT reaction was performed at 16°C for 30 min, followed by 42°C for 30 min, and 85°C for 5 min. The TaqMan Universal PCR Master Mix with no AmpErase UNG was used for PCR amplification with reaction conditions of 95°C for 10 min followed by 40 cycles at 95°C for 15 sec and 60°C for 1 min. A standard curve was generated using a synthetic RNA equivalent to mature miR-122. HCV viral RNA levels in the serum and liver were determined using a real-time, quantitative RT-PCR (TaqMan) assay detecting sequences in the viral 5' noncoding RNA using an ABI 7500 sequence detector (PE Biosystems, Foster City, CA) as previously described [30]. Synthetic HCV RNA was used to generate a standard curve for determination of genome equivalents. The forward primer was from nucleotide 149 to 167 (5'-tgcggaaccggtgagtaca-3'), the reverse primer was from nucleotide 210 to 191 (5'-cgggtttatccaagaaagga-3') and the probe was from nucleotide 189 to 169 (5'-ccggtcgtcctggcaattccg-3') in the 5' NCR of HCV.

Affymetrix array analysis

Human RNA samples were subjected to high-density oligonucleotide microarray analysis as described previously [28]. In brief, cDNA amplified using the WT-Ovation Pico RNA Amplification System (NuGen, San Carlos, CA, USA) was used for fragmentation and biotin labeling with the FL-Ovation cDNA Biotin Module V2 (NuGen). Biotin-labeled cDNA suspended in hybridization cocktail (NuGen) was hybridized to Affymetrix U133 Plus 2.0 GeneChips, followed by labeling with streptavidin-phycoerythrin. Probe hybridization was determined using a GeneChip Scanner 3000 (Affymetrix) and analyzed using GeneChip Operating Software 1.4 (Affymetrix).

Statistical analysis

Statistical analyses were carried out using Prism V software (Graphpad Software, Inc). The paired t test was used for comparison of results arising from groups of paired tissue specimens (HCC versus non-tumor tissue), while the unpaired t test or Mann-Whitney test was used for comparisons between groups of unrelated tissues (e.g., HBV versus HCV infection). Nonparametric analysis of the correlation between miR-122 and ISG expression levels was done by the Spearman method. Other statistical tests were as described in the text.

Results

miR-122 abundance in HCV- versus HBV-associated liver cancer

We measured miR-122 abundance in paired tumor and non-tumor tissues collected from 26 patients undergoing surgical resection of HCC: 16 with concomitant chronic HCV infection, and 10 infected with HBV. The age, gender, histological classification of HCC, and fibrosis score of non-tumor tissues are shown in Figure 1 (see also Table 1). Subjects infected with HCV (predominantly genotype 1b) were approximately one decade older than those with HBV infection (66.6 ± 8.0 s.d. versus 54.3 ± 9.1 s.d. years, p=0.001, Figure 1A), consistent with previous studies indicating that HCC is generally diagnosed at an earlier age in HBV-infected Japanese patients [31]. There were no significant differences in the histological classification of HCC or scores for fibrosis or inflammatory activity in non-tumor tissues between the two groups (Figure 1B and C, and Table 1). There were more females among those with HCV infection (10 male and 6 female) than HBV (9 male and 1 female), but this difference did not achieve statistical significance (Chi square test with Yate's correction).

qRT-PCR revealed significant differences in the abundance of miR-122 in both tumor and non-tumor tissue samples when the HBV- and HCV-infected groups were compared (Figure 2). miR-122 abundance (miR-122 copy number per µg total RNA) was significantly lower in HCC tissue from HBV-infected versus HCV-infected subjects (p=0.009 by two-sided t test). In contrast, the miR-122 abundance in non-tumor tissue from HBV-infected patients was significantly greater than that in the HCV-infected patients (p=0.0005 by two-sided t test). The mean miR-122 abundance in HCC tissue was less than half that in non-tumor tissue in HBV-infected patients (p=0.003 by two-sided, paired t test). Strikingly, this relationship was reversed in the HCV-infected patients, in whom miR-122 abundance in HCC tissue was almost twice that in the non-tumor tissue (p=0.008 by two-sided paired t test). There was no significant difference in the abundance of miR-122 in the non-tumor tissue from HBV-infected patients and HCV-associated

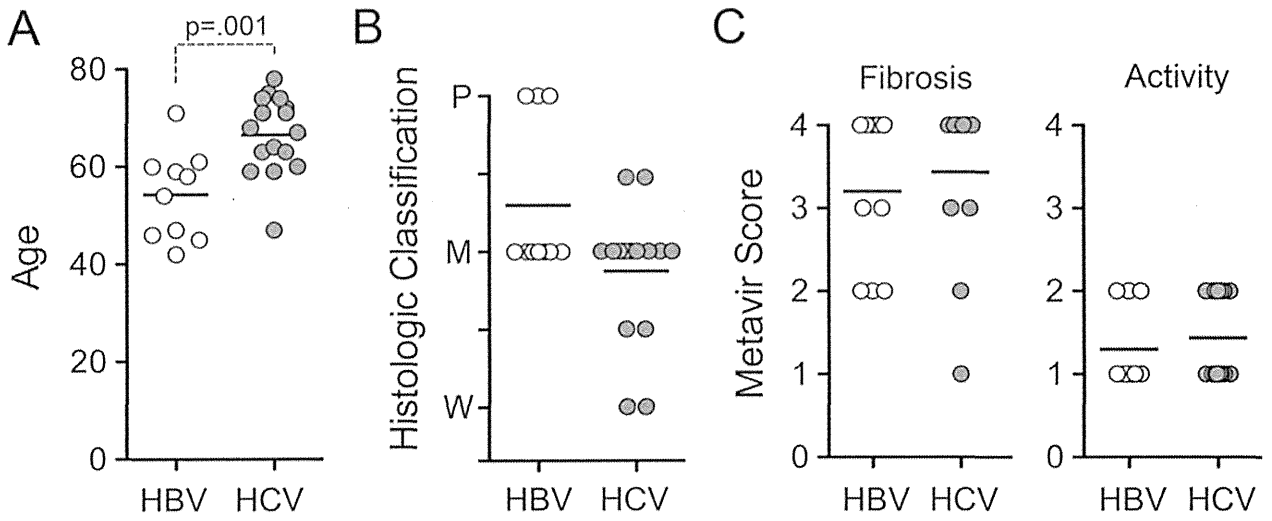

Figure 1. Age, histological classification of tumors, and scoring of non-tumor tissue for inflammation and fibrosis. (**A**) Age of subjects from whom HBV- and HCV-associated HCC and paired non-tumor samples were obtained. (**B**) Histological classification of tumors: W = well differentiated, M = moderately differentiated, P = poorly differentiated. (**C**) Individual scores for fibrosis and inflammatory activity in non-tumor tissue. Bars represent mean values. See also Table 1.

doi: 10.1371/journal.pone.0076867.g001

HCC. miR-122 abundance varied quite widely in liver tissue collected from non-infected individuals undergoing resection of metastatic tumors. Despite this, miR-122 abundance was significantly less in HBV-associated cancer tissue and non-tumor HCV-infected tissue than in the non-infected tissues (p=0.016 and 0.013, respectively).

To account for potential differences in degradation of the RNA or efficiency of reverse transcription between tissue samples, we assessed the abundance of several other small RNAs against which we could normalize the abundance of miR-122. U6, a noncoding snRNA component of the spliceosome, is commonly used to normalize miRNA abundance. However, we observed substantial differences in U6 abundance in these tissues, suggesting that U6 would be a poor normalizer (Figure 3A). Substantially less variation was observed in the abundance of the miRNAs, miR-24 or Let-7a (Figure 3B and C), for which the standard deviation of the critical threshold [25] in the PCR assay was 0.79 and 1.27, respectively, compared to 1.34 for U6. Notably, we observed no difference in the abundance of Let-7a in HBV-associated cancer and non-tumor tissues (p=0.52 by two-sided, paired t test), despite a prior report suggesting that Let-7a expression is regulated by the HBx protein and increased in abundance in HBV-associated HCC [32]. In addition, although miR-24 negatively regulates the expression of hepatocyte nuclear factor 4-alpha (HNF4-alpha) and thus might be up-regulated in some liver cancers [33], we did not observe this. A strong positive correlation was evident between the abundance of miR-24 and Let-7a (Figure 3E, Spearman r_s=0.7959, p<0.001 by two-tailed t test), suggesting that these miRNAs might belong to a common regulatory network and that either could be used to normalize miR-122 abundance. In contrast, there was no correlation between miR-24 and either U6 or miR-122 abundance (Figure 3D and F), which indicates that U6 and miR-122 are regulated independently of miR-24. Importantly, when the miR-122 abundance was normalized to miR-24 levels, miR-122 expression remained significantly depressed in HBV-associated HCC when compared either with paired non-tumor tissue, or HCC tissue from HCV-infected subjects (p<0.001 and p=0.002, respectively, Figure 2B). In replicate assays, the abundance of miR-122 in non-tumor HCV-infected tissue also remained significantly lower than either non-infected or HBV-infected liver tissues (Figure 2B). Similar associations were found when miR-122 abundance was normalized to Let-7a (data not shown).

To assess further the possibility of bias in these results due to differences in the quality of the RNA samples, we compared the RNA integrity number (RIN) [29] of each sample with the abundance of each of the small RNAs detected. Interestingly, while the quantity of U6 snRNA detected correlated positively with the RIN score (Spearman r_s = 0.5216, two-tailed p = 0.0001) (Figure S1A in Supporting Information), this was not the case with miR-24 or Let-7a (r_s = -0.124 and -0.045, respectively). RIN scores also did not vary significantly between tumor and non-tumor tissue-derived RNA samples, or RNA from HBV- vs. HCV-infected tissue. Thus, although the quality of the RNA samples was generally high (mean RIN = 8.0 ± 0.17 s.e.m.), it was an important factor in determining the abundance of U6 but not either of these miRNAs. These data suggest that U6 is less stable than the miRNAs and provide additional support for the use of miR-24 (or Let-7a) as a standard against which to normalize miR-122 abundance (see Discussion). Nonetheless, when miR-122 results were normalized to U6 abundance, the correlations described above

Table 1. Characteristics of Study Subjects.

	HCV (n = 16)	HBV (n=10)	Non-infected (n=9)
Mean Age (years)	66.6 ± 8.0 s.d.	54.3 ± 9.1	60.1 ± 14.3
Gender (M/F)	10M/6F	9M / 1F	5M / 4F
HCV Genotype			
1a	0	n/a	n/a
1b	14		
2	2		
3	0		
Fibrosis Stage	n (%)	n (%)	n (%)
0	0 (0)	0 (0)	9 (100)
1	1 (6)	0 (0)	0 (0)
2	1 (6)	3 (30)	0 (0)
3	4 (25)	2 (20)	0 (0)
4	10 (63)	5 (50)	0 (0)
Inflammation	n (%)	n (%)	n (%)
0	0 (0)	0 (0)	9 (100)
1	9 (56)	7 (70)	0 (0)
2	7 (44)	3 (30)	0 (0)
3	0 (0)	0 (0)	0 (0)
4	0 (0)	0 (0)	0 (0)
HCC Histologic Differentiation	n (%)	n (%)	
Well	2 (13)	0 (0)	n/a
Moderate-Well	2 (13)	0 (0)	
Moderate	10 (63)	7 (30)	
Poor-Moderate	2 (13)	0	
Poor	0 (0)	3 (30)	
IL28B genotype (rs8099917)	n (%)		
TT	9 (56)	n.d.	n.d.
TG	7 (44)		
GG	0 (0)		

n/a = "not applicable"; n.d. = "not done"

doi: 10.1371/journal.pone.0076867.t001

between miR-122 abundance, in both tumor and non-tumor tissues, and the type of virus infection remained strongly statistically significant (Figure S1B in Supporting Information). The mean miR-122 abundance was substantially lower in HBV-associated HCC tissue than in HBV-infected non-tumor tissue ($p = 0.003$ by paired t-test), while this relationship was reversed in HCV-infected liver ($p = 0.001$). miR-122 abundance was also significantly lower in non-tumor tissue from HCV-infected subjects than HBV-infected subjects ($p < 0.001$).

To exclude the possibility of bias due to the trend toward a less differentiated histologic classification among HBV-associated cancers (Figure 1B), we limited the comparison of miR-122 abundance to those HCC tissues that were scored as moderately differentiated and their corresponding paired non-tumor samples. While this reduced the number of subjects available for analysis, miR-122 abundance remained significantly lower in HBV- versus HCV-associated cancer tissue: $p=0.007$ when compared on the basis of miR-122 copy number/mg RNA (Figure 2C) vs. $p=0.033$ when normalized to miR-24 (Figure 2D). Thus differences in miR-122 abundance in HCC associated with HBV vs. HCV infection are independent of the degree of histologic differentiation of the cancer.

Collectively, these results provide strong evidence that miR-122 expression is reduced in HCC associated with HBV infection, but not in most HCV-associated liver cancers.

Reduced miR-122 abundance is associated with interferon responses in HCV-infected liver

The data shown in Figure 2 indicate that miR-122 is frequently reduced in abundance in non-tumor, HCV-infected liver tissue, but not in liver infected with HBV. To determine whether similar HCV-induced suppression of miR-122 expression occurs in chimpanzees (*Pan troglodytes*), the only animal species other than humans that is permissive for HCV infection, we measured miR-122 abundance in liver tissues

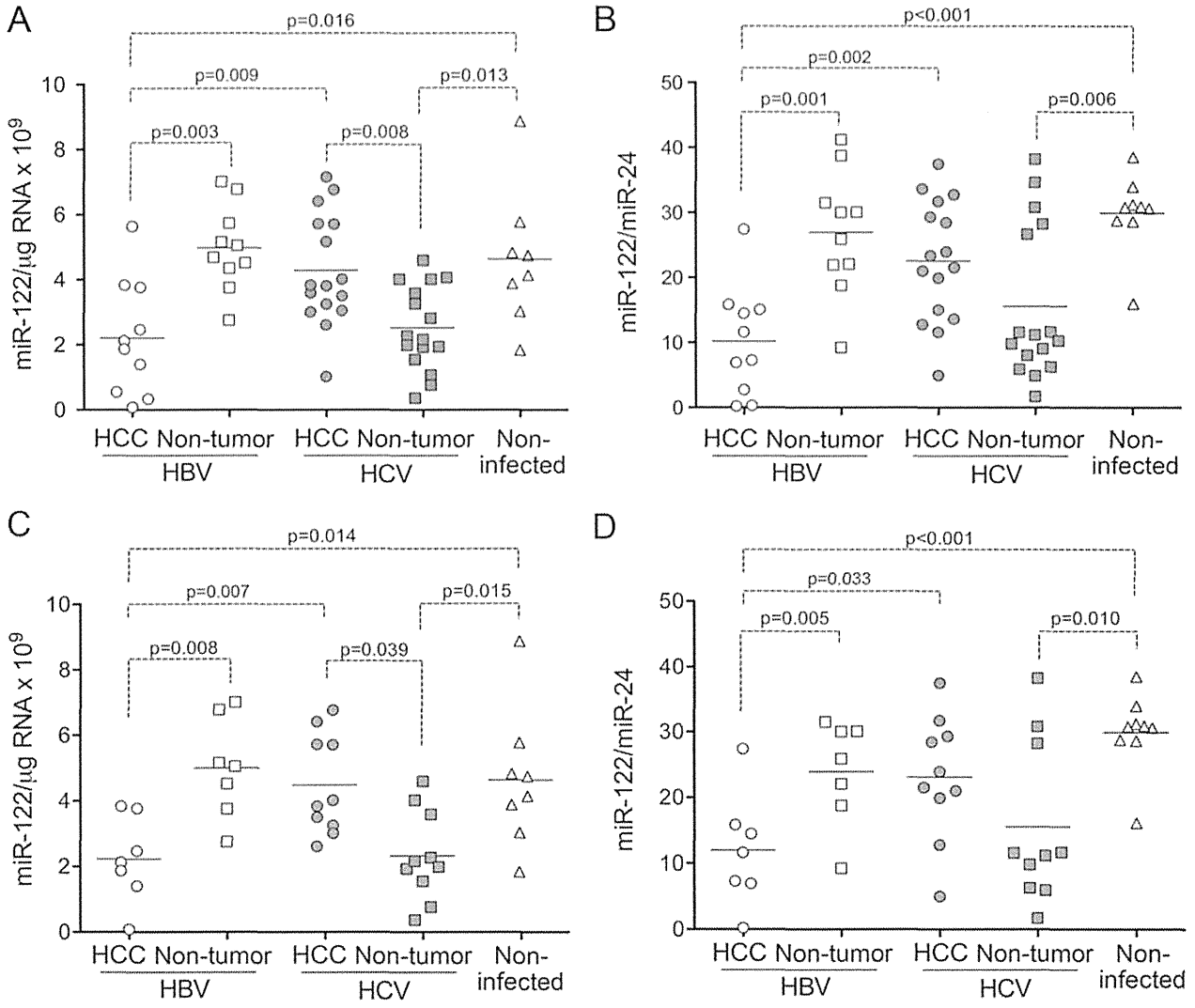

Figure 2. miR-122 expression in paired HCC and non-tumor liver tissue from patients with chronic HBV and HCV infection and control, non-infected liver tissue. (**A**) miR-122 abundance quantified by qRT-PCR in paired tumor and non-tumor tissues and non-infected ('normal') liver from patients undergoing resection of metastatic tumors, normalized to total RNA. (**B**) Relative miR-122 abundance normalized to miR-24 abundance in the same tissues. (**C**) miR-122 abundance in HCC classified histologically as "moderately differentiated", paired non-tumor tissue from the same patients, and non-infected ('normal') liver. (**D**) miR-122 abundance in the subset of tissues shown in panel C, normalized to miR-24 abundance. The statistical significance of differences between paired observations was estimated using the paired t test, while differences between non-paired observations were analyzed by the Mann-Whitney test.

doi: 10.1371/journal.pone.0076867.g002

collected previously from 45 HCV-infected chimpanzees, and compared this to that present in 10 HBV-infected animals, and 6 that were not infected with either virus. These results showed that miR-122 expression was significantly reduced in HCV-infected liver compared to both HBV-infected ($p<0.0001$) and normal, non-infected ($p=0.007$) chimpanzee liver (Figure 4A). A strong, negative correlation (Spearman $r_s= -0.63$, $p<0.0001$) existed between hepatic miR-122 expression levels and HCV RNA copy numbers in serum (Figure 4B). The mean miR-122 abundance was lower in HBV-infected liver than in uninfected chimpanzee liver (Figure 4A), but the difference did not achieve statistical significance ($p=0.059$ by two-tailed t test). Thus, intra-hepatic miR-122 abundance is reduced in HCV-infected chimpanzees as well as humans. This is consistent with earlier studies that have found reduced intrahepatic expression of miR-122 in patients with advanced chronic hepatitis C [34–36].

Sarasin-Filipowicz et al. [36] reported previously that miR-122 levels were reduced in liver from HCV-infected

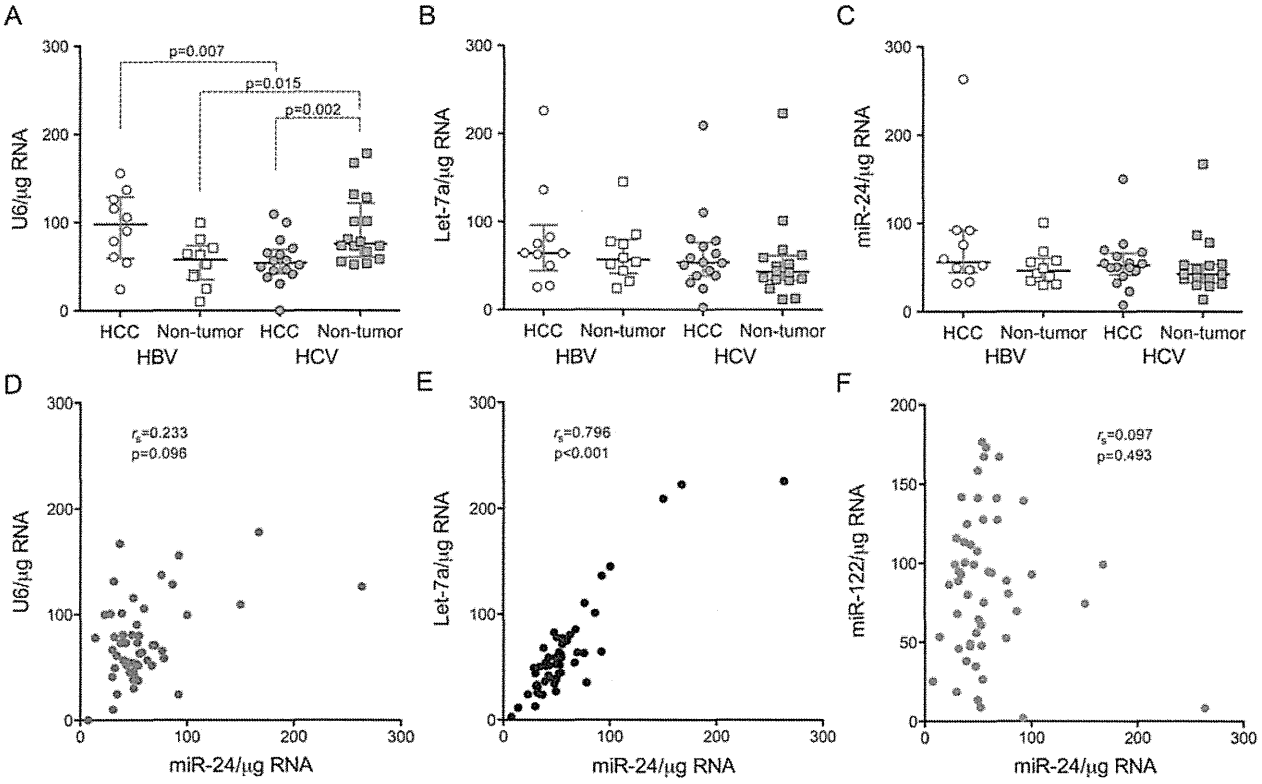

Figure 3. Comparison of small RNAs as normalizers for assessing miR-122 abundance. Shown in the panels at the top are the relative abundance of (**A**) U6 snRNA, (**B**) Let-7a, and (**C**) miR-24 miRNAs in paired tumor and non-tumor tissues from subjects with HBV or HCV infection, normalized to total RNA. Bars represent median and quartiles for each group. Statistical comparisons between groups were made with paired or unpaired t tests, and are shown only if p<.05. In the lower set of panels, (**D**) U6, (**E**) Let-7a, and (**F**) miR-122 abundance are plotted as a function of miR-24 abundance. r_s = Spearman rank-order correlation coefficient.

doi: 10.1371/journal.pone.0076867.g003

patients who responded poorly to treatment with pegylated IFN-α and ribavirin (Peg-IFN/RBV). Consistent with this, we observed a negative correlation between miR-122 abundance in non-tumor tissue from HCV-infected human subjects and the GT versus TT genotype at the rs8099917 locus in the IL28B gene (p=0.011, Figure 5A) that is predictive of a poor response to Peg-IFN/RBV therapy [37]. HCV-infected patients with the TT genotype are prone to a greater inflammatory response than those with TG or GG [38]. Thus, differences in IL28B genotype may have contributed to a correlation we observed between miR-122 abundance and A1 versus A2 Metavir activity scores (Figure 5B, 6 of 7 subjects with an A2 Metavir score had the TT genotype). Importantly, the association between IL28B genotype and miR-122 abundance was observed only in non-tumor liver from HCV-infected patients, and not in paired HCC tissue (Figure 5A).

Patients who are non-responsive to Peg-IFN/RBV, or who have IL28B genotypes predictive of a poor response to Peg-IFN/RBV therapy, are likely to have increased pre-treatment intra-hepatic ISG transcript levels compared to those who respond well to treatment [39–41]. We thus asked whether a correlation existed between miR-122 abundance and levels of selected ISG transcripts in HCV-infected non-tumor tissue determined by Affymetrix 133U Plus 2.0 GeneChip assay. For this analysis, we selected ISGs that were shown previously to be correlated with treatment response [39] (Figure 5C). We also included Mx1 and OAS1, both well-characterized ISGs. Overall, the Affymetrix signals for these genes showed a strong trend toward negative correlations with miR-122 abundance. Fourteen of 24 ISGs demonstrated a Spearman rank-order coefficient, r_s, ≤ -0.300; this negative correlation was significant (p<0.05) for 7 of the ISGs by one-tailed t test (Figure 3C). These data are consistent with the notion that reduced miR-122 abundance is associated with strong intrahepatic IFN-mediated responses to the virus.

miR-191 abundance is increased in HBV-associated HCC

Since Elyakim et al. [42] reported recently that miR-191 was increased in HCC arising in a study population comprised mostly of HBV-infected subjects, we also quantified miR-191 expression levels in the human tissue samples. We confirmed

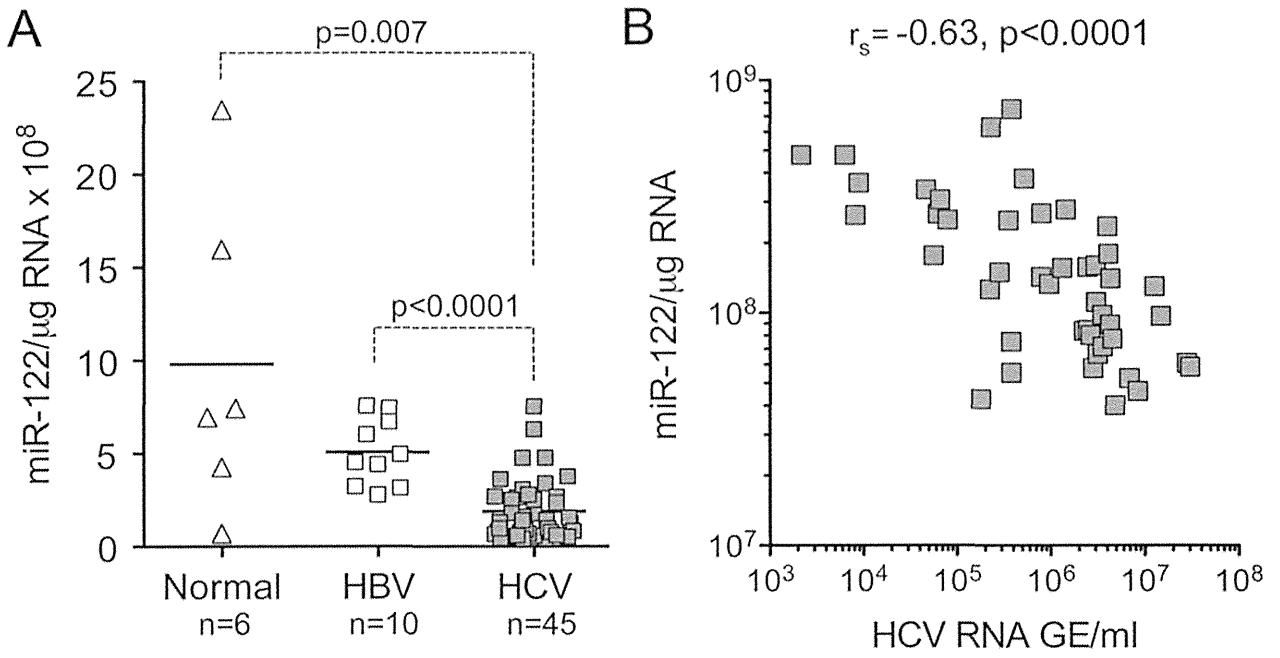

Figure 4. miR-122 expression in chimpanzee liver tissue. (**A**) Hepatic miR-122 abundance in liver biopsies from chimpanzees infected with HBV or HCV, or not infected with either virus ('normal'). Statistical significance was assessed by non-paired two-sided t test. Bars represent mean values. (**B**) Liver miR-122 expression plotted against serum HCV RNA abundance from acutely HCV-infected chimpanzees. r_s = Spearman rank-order correlation coefficient.

doi: 10.1371/journal.pone.0076867.g004

miR-191 levels were modestly increased in HBV-associated HCC compared to non-tumor HBV-infected tissue when normalized to total RNA (p=0.049 by two-sided, paired t test, Figure 6). This trend remained significant only by one-sided t test when the miR-191 abundance was normalized to miR-24 abundance (p=0.045), and was absent when miR-191 levels were normalized to U6 snRNA. miR-191 abundance in non-tumor, HBV-infected tissue was similar to that in both tumor and non-tumor liver from HCV-infected subjects (Figure 6).

Discussion/Conclusions

miR-122 is a critical regulator of hepatic gene expression and an essential host factor for HCV replication [15,18,43]. It also has important tumor suppressor properties [16,44], and recent reports indicate that loss of its expression promotes carcinogenesis in knockout mice [45,46]. While its abundance is often reduced in HCC [21,22], two previous studies suggest that miR-122 expression may be preserved in liver cancer arising in patients with HCV infection [24,25]. We confirm this, showing in a genetically and geographically homogeneous population of patients, and normalizing results either to total RNA or to levels of miR-24, that miR-122 abundance is significantly reduced from normal in HBV-associated HCC but not in liver cancer associated with HCV infection (Figure 2A and B). This difference in miR-122 expression is independent of the histologic classification of the tumors (Figure 2C and D), as well as the degree of fibrosis or inflammation in paired non-tumor tissue from the same patients. Conversely, we show that miR-191 tends to be increased in abundance in HBV-associated cancer, but not HCV-associated HCC (Figure 6). These observations have important implications for the pathogenetic mechanisms involved in viral carcinogenesis within the liver. While HCC may arise as a result of factors common to both HBV and HCV infection (such as chronic inflammation, oxidative stress, and progressive fibrosis leading to cirrhosis), distinctive molecular signatures associated with HBV- versus HCV-associated cancer suggest there are fundamental differences in the ways these two viruses cause cancer.

Our study highlights the challenges inherent in comparing miRNA abundance in different clinical samples. In addition to potential differences in the proportion of cells present within a biopsy that are of hepatocellular origin vs. derived from other cell lineages, a constant concern is the quality of the RNA. While our initial analysis, like many studies, compared miR-122 copy numbers based on the quantity of total RNA subjected to RT-PCR, this approach can be biased by differences in the quality of the RNA and degree of RNA degradation. Although our RNA samples were of generally high quality (see Figure S1A in Supporting Information), we determined miR-24, Let-7a, and U6 snRNA copy numbers and evaluated each as a standard against which miR-122 abundance could be normalized to account for potential differences in RNA integrity (Figure 3). Median miR-24 and Let-7a copy numbers did not

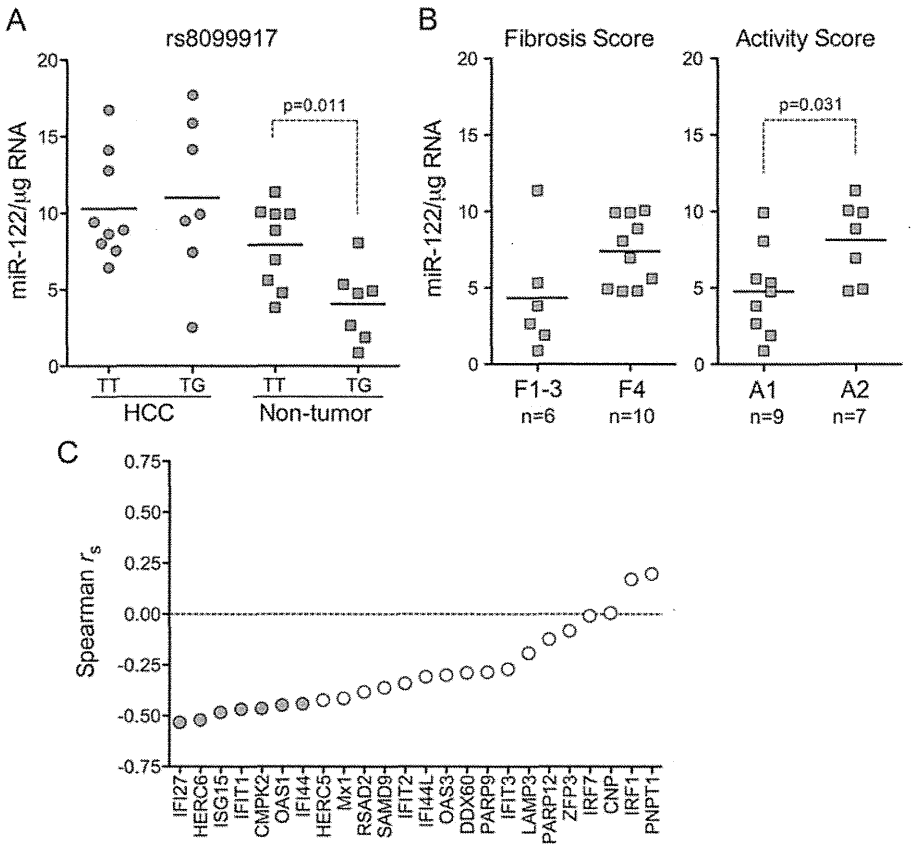

Figure 5. miR-122 expression, IL28B genotype, Metavir scores and ISG transcript levels in HCV-infected human liver. (**A**) miR-122 expression in HCC and paired non-tumor samples from subjects with HCV infection, grouped according to rs8099917 genotype (TT or GT). (**B**) miR-122 expression levels in non-tumor tissue from HCV-infected subjects categorized according to Metavir score for (left) fibrosis and (right) inflammatory activity. (**C**) Correlation between miR-122 abundance and expression levels of selected ISGs determined by Affymetrix U133 Plus 2.0 Array analysis. With the exception of OAS1 and Mx1, intrahepatic transcript levels of these ISGs have been shown previously to be predictive of Peg-IFN/RBV treatment outcome [31]. "r_s" = Spearman rank-order correlation coefficient. Filled symbols indicate a statistically significant negative correlation ($p<0.05$ by one-sided t test).

doi: 10.1371/journal.pone.0076867.g005

vary significantly between tumor and non-tumor tissue samples from HBV- and HCV-infected subjects (one-way ANOVA), suggesting that the expression of these miRNAs is relatively constant in liver and that either could serve as a standard for normalizing miR-122 abundance. In contrast, median U6 copy numbers varied significantly between these tissue groups ($p = 0.004$ by one-way ANOVA with Kruskal-Wallis test) and, more importantly, were strongly correlated negatively with the RIN score, a measure of RNA integrity [29] (Figure S1A in Supporting Information). There was no correlation between the RIN score and miR-24 or Let-7a abundance, suggesting that U6 snRNA may be less stable and more prone to degradation than the miRNAs. This may be due to the greater length of U6 (106 nts vs. ~20-23 nts for miRNAs), or the absence of terminal modifications that may influence the stability of miRNAs [47]. Consistent with this, Let-7a was found to have greater biological stability and to be superior to U6 for normalization of miRNA abundance in previous studies of rat hepatocyte RNA [48]. Nonetheless, even though these data argue against the use of U6 as a standard for normalizing miR-122 copy numbers, we found the abundance of miR-122 was significantly reduced in HCC associated with HBV but not HCV infection, and that miR-122 abundance was significantly depressed in non-tumor tissue infected with HCV but not HBV, using any of these small RNAs, including U6, to normalize the miR-122 results.

While it remains unclear exactly how miR-122 contributes to the HCV lifecycle, it is known to promote viral replication independently of its regulation of hepatic genes [49]. It binds to two sites near the 5' end of the viral genome [18], recruiting argonaute 2 (EIF2C2) and physically stabilizing the RNA by protecting it from 5' exonucleolytic Xrn1-mediated decay [19,20]. However, miR-122 has other, positive effects on HCV replication beyond its ability to physically stabilize the viral

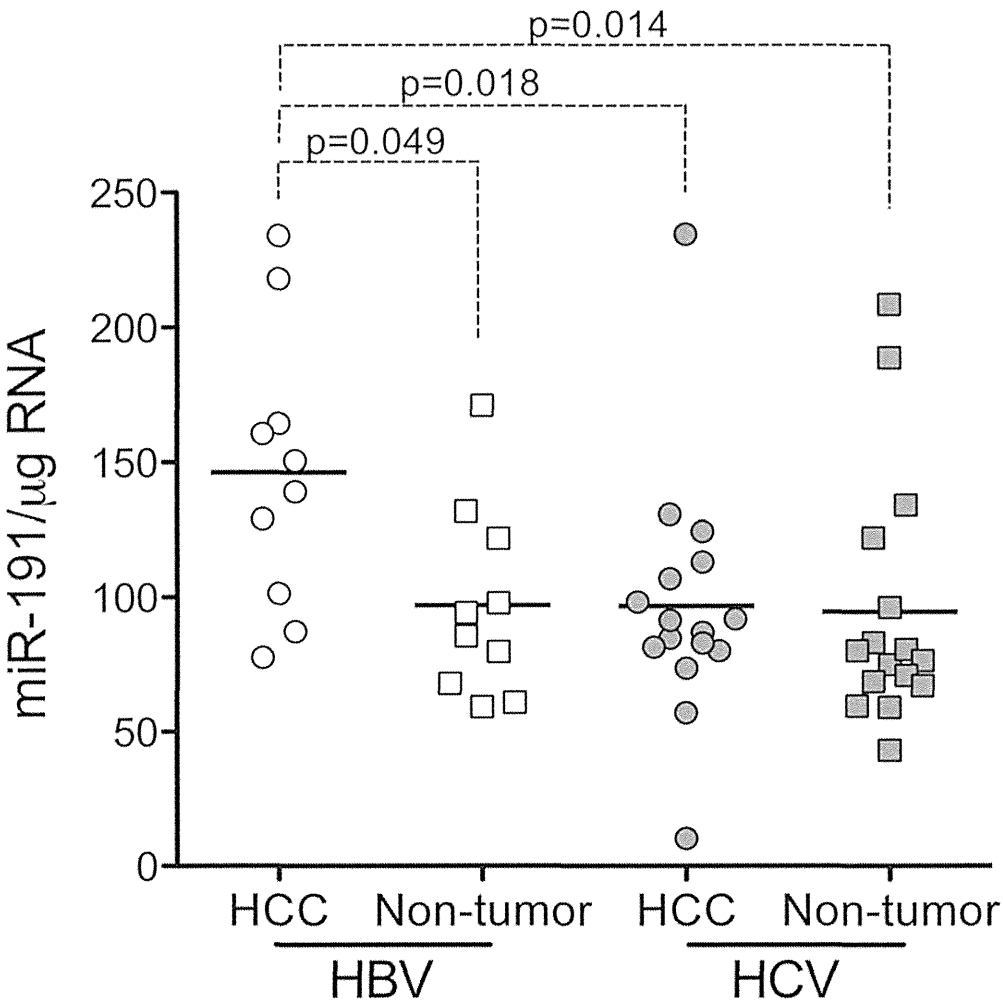

Figure 6. Relative abundance of miR-191 in paired HCC and non-tumor tissue from subjects with HBV or HCV infection. Relative miR-191 abundance in paired tumor and non-tumor samples from HBV- and HCV-infected subjects normalized to total RNA. Statistical significance was assessed in two-sided paired t tests for comparisons between tumor and non-tumor tissue, or two-sided unpaired t test for comparison between infection groups.

doi: 10.1371/journal.pone.0076867.g006

genome [20,50]. It is essential for HCV replication, and its therapeutic silencing with an antisense oligonucleotide has potent antiviral effects [15,51]. No other RNA virus is known to rely so completely on a cellular miRNA for its replication cycle. Thus, the continued expression of miR-122 in HCV-associated HCC could reflect close linkage between carcinogenesis and HCV replication and viral protein expression. We speculate that miR-122 expression is preserved in HCV-associated HCC (in contrast to HBV-associated cancer) because HCV-encoded proteins help to drive a multi-stage process of carcinogenesis within infected cells. This may result from the ability of the virus to directly disable DNA damage responses or other cellular tumor suppressor functions, and to contribute directly to malignant conversion of hepatocytes as reviewed elsewhere [10,52]. Early loss of miR-122 during the progression to cancer would eliminate virus replication, protecting the cell from further effects of viral protein expression. In contrast, in HBV-infected cells, a loss of miR-122 expression could both accelerate tumorigenesis and enhance replication, as miR-122 appears to restrict, rather than promote, HBV replication [53–56]. Although speculative, this hypothesis raises the interesting possibility that HCV-associated cancers arise within the small minority of hepatocytes infected with the virus, and not the much larger number of uninfected bystander cells [52,57].

Epigenetic mechanisms are likely to contribute to the differential expression of miR-122 and miR-191 in HCC. The miR-122 promoter is hyper-methylated in the HBV-associated HCC-derived cell line, Hep3B [58]. It remains to be seen whether differences exist in methylation of the promoter in vivo in HBV- versus HCV-associated cancers, but bacterial artificial

chromosome array-based methylated CpG island amplification (BAMCA) studies indicate significant differences in the methylation patterns present in HBV- and HCV-associated HCC [59]. The HBx protein expressed by HBV may influence cellular methyltransferase activity, and could possibly contribute to altered methylation patterns [60]. An additional possibility is that epigenetic differences in HBV- and HCV-associated HCC could reflect different cell types from which the cancer originates, as HBV may be capable of infecting hepatocyte progenitors [61].

Our results also show that miR-122 expression is reduced in non-tumor liver tissue from HCV-infected persons. In contrast, contrary to a recent report by Wang et al. [54], we found that miR-122 is expressed at normal levels in non-tumor HBV-infected liver (Figure 2). Several lines of evidence suggest that this difference may reflect a more active IFN response in HCV- versus HBV- infected livers. In vitro studies suggest that IFN-β inhibits miR-122 expression [36,62], and HCV stimulates a more robust intrahepatic innate immune response than HBV [63,64]. Consistent with this, our results reveal a correlation between miR-122 abundance in non-tumor tissues and IL28B genotype, defined by a single nucleotide polymorphism (rs8099917) associated with response to Peg-IFN/RBV as well as endogenous pre-treatment ISG expression levels (Figure 5A) [40,41]. We also found an inverse relationship between the abundance of several ISG transcripts and miR-122 (Figure 5C). Interestingly, this relationship was not observed in tumor tissues from these patients, suggesting that genetic or epigenetic changes alter miR-122 regulation in HCC tissue, or that the cancer cells are refractory to stimulation by type 1 IFNs.

Consistent with our findings in HCV-infected patients, we also observed a reduction in miR-122 abundance in liver tissue from HCV-infected chimpanzees (Figure 4A), and an inverse correlation between the abundance of HCV RNA in the liver and serum HCV RNA levels (Figure 4B). Although Sarasin-Filopowicz et al. [36] demonstrated a trend toward lower miR-122 abundance in liver tissues with high viral RNA copy numbers, this did not achieve statistical significance and no correlation was evident between serum RNA levels and miR-122 abundance in the patients studied by this group. It is not clear why such a relationship exists in chimpanzees but not infected humans. One possibility is that it might be related to the fact that chimpanzees generally have very robust intrahepatic innate immune responses to HCV, with uniformly high levels of intrahepatic ISG expression [65]. The uniformly high intrahepatic innate immune response in chimpanzees contrasts with extensive variation in the intensity of ISG responses in HCV-infected humans [39], possibly allowing for a negative correlation between serum viral RNA level and miR-122 abundance to become manifest.

Finally, our results indicate that miR-191 expression may be increased in HBV-associated HCC (Figure 6). This supports a previous study in which miR-191 abundance was increased in HCC of mixed origin, but predominantly associated with HBV infection [42]. miR-191 antagonism has been shown to have anti-tumor potential in studies of Hep3B and SNU423 cells [42], which are both derived from HBV-associated cancers. Our data suggest that elevations of miR-191 are confined to HBV-associated liver cancer (Figure 6), and suggest that virus-specific differences in miRNA signatures may be important in understanding the origins of liver cancer. While these differences may be predictive of response to specific therapeutic interventions, they are unlikely to be of sufficient magnitude or specificity to guide therapy in individual patients.

Supporting Information

Figure S1. U6 snRNA copy number as a standard for normalization of miR-122 abundance. (**A**) U6 copy number (relative copy number per μg RNA) plotted as a function of the RNA integrity number (RIN score, on a scale of 1 to 10) determined as described in Methods in the main text. A strong negative correlation exists between U6 copy number and the RIN score: Spearman r_s = 0.5216, two-tailed p = 0.0001). (**B**) miR-122 abundance in HCC and non-tumor tissues from HBV- and HCV-infected subjects, normalized to U6 snRNA copy number. Statistical significance was assessed using paired and unpaired t tests, as described in the main text.
(TIF)

Author Contributions

Conceived and designed the experiments: CS MH SRS REL SML. Performed the experiments: CS SRS DY TS. Analyzed the data: CS MH SRS DY REL SML. Contributed reagents/materials/analysis tools: MH SK REL. Wrote the manuscript: CS SML.

References

1. Ferlay JSH, Bray F, Forman D, Mathers C, Parkin DM (2010). ancer Incidence Mortal Worldwide IARC CancerBase No. 10
2. Wang XGJ, Thorgeirsson S, editors (2011) Molecular Genetics of Liver Neoplasia. New York: Springer Verlag Science. pp. 51-73.
3. Lok AS, Everhart JE, Wright EC, Di Bisceglie AM, Kim HY et al. (2011) Maintenance peginterferon therapy and other factors associated with hepatocellular carcinoma in patients with advanced hepatitis C. Gastroenterology 140: 840-849. doi:10.1053/j.gastro.2010.11.050. PubMed: 21129375.
4. White D, El-Serag H (2011) Epidemiology of Hepatocellular Carcinoma. In: X Wang[!(surname)!]S Thorgeirsson. Molecular Genetics of Liver Neoplasia. New York, NY: Springer Verlag Science. pp. 51-73.
5. Kiyosawa K, Umemura T, Ichijo T, Matsumoto A, Yoshizawa K et al. (2004) Hepatocellular carcinoma: recent trends in Japan. Gastroenterology 127: S17-S26. doi:10.1053/j.gastro.2004.03.068. PubMed: 15508082.
6. McGivern DR, Lemon SM (2011) Virus-specific mechanisms of carcinogenesis in hepatitis C virus associated liver cancer. Oncogene 30: 1969-1983. doi:10.1038/onc.2010.594. PubMed: 21258404.
7. Tsai WL, Chung RT (2010) Viral hepatocarcinogenesis. Oncogene 29: 2309-2324. doi:10.1038/onc.2010.36. PubMed: 20228847.
8. Nakamoto Y, Guidotti LG, Kuhlen CV, Fowler P, Chisari FV (1998) Immune pathogenesis of hepatocellular carcinoma. J Exp Med 188: 341-350. doi:10.1084/jem.188.2.341. PubMed: 9670046.
9. Lerat H, Honda M, Beard MR, Loesch K, Sun J et al. (2002) Steatosis and liver cancer in transgenic mice expressing the structural and nonstructural proteins of hepatitis C virus. Gastroenterology 122: 352-365. doi:10.1053/gast.2002.31001. PubMed: 11832450.

10. McGivern DR, Lemon SM (2009) Tumor suppressors, chromosomal instability, and hepatitis C virus-associated liver cancer. Annu Rev Pathol 4: 399-415. doi:10.1146/annurev.pathol.4.110807.092202. PubMed: 18928409.
11. Wilson RC, Doudna JA (2013) Molecular mechanisms of RNA interference. Annu Rev Biophys 42: 217-239. doi:10.1146/annurev-biophys-083012-130404. PubMed: 23654304.
12. Djuranovic S, Nahvi A, Green R (2011) A parsimonious model for gene regulation by miRNAs. Science 331: 550-553. doi:10.1126/science.1191138. PubMed: 21292970.
13. Meijer HA, Kong YW, Lu WT, Wilczynska A, Spriggs RV et al. (2013) Translational repression and eIF4A2 activity are critical for microRNA-mediated gene regulation. Science 340: 82-85. doi:10.1126/science.1231197. PubMed: 23559250.
14. Chang J, Nicolas E, Marks D, Sander C, Lerro A et al. (2004) miR-122, a mammalian liver-specific microRNA, is processed from hcr mRNA and may downregulate the high affinity cationic amino acid transporter CAT-1. RNA Biol 1: 106-113. doi:10.4161/rna.1.2.1066. PubMed: 17179747.
15. Lanford RE, Hildebrandt-Eriksen ES, Petri A, Persson R, Lindow M et al. (2010) Therapeutic silencing of microRNA-122 in primates with chronic hepatitis C virus infection. Science 327: 198-201. doi:10.1126/science.1178178. PubMed: 19965718.
16. Bai S, Nasser MW, Wang B, Hsu SH, Datta J et al. (2009) MicroRNA-122 inhibits tumorigenic properties of hepatocellular carcinoma cells and sensitizes these cells to sorafenib. J Biol Chem 284: 32015-32027. doi:10.1074/jbc.M109.016774. PubMed: 19726678.
17. Lewis AP, Jopling CL (2010) Regulation and biological function of the liver-specific miR-122. Biochem Soc Trans 38: 1553-1557. doi:10.1042/BST0381553. PubMed: 21118125.
18. Jopling CL, Yi M, Lancaster AM, Lemon SM, Sarnow P (2005) Modulation of hepatitis C virus RNA abundance by a liver-specific MicroRNA. Science 309: 1577-1581. doi:10.1126/science.1113329. PubMed: 16141076.
19. Shimakami T, Yamane D, Jangra RK, Kempf BJ, Spaniel C et al. (2012) Stabilization of hepatitis C virus RNA by an Ago2-miR-122 complex. Proc Natl Acad Sci U S A 109: 941-946. doi:10.1073/pnas.1112263109. PubMed: 22215596.
20. Li Y, Masaki T, Yamane D, McGivern DR, Lemon SM (2013) Competing and noncompeting activities of miR-122 and the 5' exonuclease Xrn1 in regulation of hepatitis C virus replication. Proc Natl Acad Sci U S A 110: 1881-1886. doi:10.1073/pnas.1213515110. PubMed: 23248316.
21. Kutay H, Bai S, Datta J, Motiwala T, Pogribny I et al. (2006) Downregulation of miR-122 in the rodent and human hepatocellular carcinomas. J Cell Biochem 99: 671-678. doi:10.1002/jcb.20982. PubMed: 16924677.
22. Gramantieri L, Ferracin M, Fornari F, Veronese A, Sabbioni S et al. (2007) Cyclin G1 is a target of miR-122a, a microRNA frequently down-regulated in human hepatocellular carcinoma. Cancer Res 67: 6092-6099. doi:10.1158/0008-5472.CAN-06-4607. PubMed: 17616664.
23. Hou J, Lin L, Zhou W, Wang Z, Ding G et al. (2011) Identification of miRNomes in human liver and hepatocellular carcinoma reveals miR-199a/b-3p as therapeutic target for hepatocellular carcinoma. Cancer Cell 19: 232-243. doi:10.1016/j.ccr.2011.01.001. PubMed: 21316602.
24. Varnholt H, Drebber U, Schulze F, Wedemeyer I, Schirmacher P et al. (2008) MicroRNA gene expression profile of hepatitis C virus-associated hepatocellular carcinoma. Hepatology 47: 1223-1232. PubMed: 18307259.
25. Coulouarn C, Factor VM, Andersen JB, Durkin ME, Thorgeirsson SS (2009) Loss of miR-122 expression in liver cancer correlates with suppression of the hepatic phenotype and gain of metastatic properties. Oncogene 28: 3526-3536. doi:10.1038/onc.2009.211. PubMed: 19617899.
26. Bedossa P, Poynard T (1996) An algorithm for the grading of activity in chronic hepatitis C. The METAVIR Cooperative Study Group. Hepatology 24: 289-293. doi:10.1002/hep.510240201. PubMed: 8690394.
27. Desmet VJ, Gerber M, Hoofnagle JH, Manns M, Scheuer PJ (1994) Classification of Chronic Hepatitis: Diagnosis, Grading and Staging. Hepatology 19: 1513-1520. doi:10.1002/hep.1840190629. PubMed: 8188183.
28. Honda M, Sakai A, Yamashita T, Nakamoto Y, Mizukoshi E et al. (2010) Hepatic ISG expression is associated with genetic variation in interleukin 28B and the outcome of IFN therapy for chronic hepatitis C. Gastroenterology 139: 499-509. doi:10.1053/j.gastro.2010.04.049. PubMed: 20434452.
29. Schroeder A, Mueller O, Stocker S, Salowsky R, Leiber M et al. (2006) The RIN: an RNA integrity number for assigning integrity values to RNA measurements. BMC Mol Biol 7: 3. doi:10.1186/1471-2199-7-3. PubMed: 16448564.
30. Lanford RE, Guerra B, Lee H, Averett DR, Pfeiffer B et al. (2003) Antiviral effect and virus-host interactions in response to alpha interferon, gamma interferon, poly(i)-poly(c), tumor necrosis factor alpha, and ribavirin in hepatitis C virus subgenomic replicons. J Virol 77: 1092-1104. doi:10.1128/JVI.77.2.1092-1104.2003. PubMed: 12502825.
31. Nagaoki Y, Hyogo H, Aikata H, Tanaka M, Naeshiro N et al. (2012) Recent trend of clinical features in patients with hepatocellular carcinoma. Hepatol Res 42: 368-375. doi:10.1111/j.1872-034X.2011.00929.x. PubMed: 22151896.
32. Wang Y, Lu Y, Toh ST, Sung WK, Tan P et al. (2010) Lethal-7 is down-regulated by the hepatitis B virus x protein and targets signal transducer and activator of transcription 3. J Hepatol 53: 57-66. doi:10.1016/j.jhep.2009.12.043. PubMed: 20447714.
33. Hatziapostolou M, Polytarchou C, Aggelidou E, Drakaki A, Poultsides GA et al. (2011) An HNF4alpha-miRNA inflammatory feedback circuit regulates hepatocellular oncogenesis. Cell 147: 1233-1247. doi:10.1016/j.cell.2011.10.043. PubMed: 22153071.
34. Trebicka J, Anadol E, Elfimova N, Strack I, Roggendorf M et al. (2013) Hepatic and serum levels of miR-122 after chronic HCV-induced fibrosis. J Hepatol 58: 234-239. doi:10.1016/S0168-8278(13)60572-3. PubMed: 23085648.
35. Morita K, Taketomi A, Shirabe K, Umeda K, Kayashima H et al. (2011) Clinical significance and potential of hepatic microRNA-122 expression in hepatitis C. Liver Int 31: 474-484. doi:10.1111/j.1478-3231.2010.02433.x. PubMed: 21199296.
36. Sarasin-Filipowicz M, Krol J, Markiewicz I, Heim MH, Filipowicz W (2009) Decreased levels of microRNA miR-122 in individuals with hepatitis C responding poorly to interferon therapy. Nat Med 15: 31-33. doi:10.1038/nm.1902. PubMed: 19122656.
37. Tanaka Y, Nishida N, Sugiyama M, Kurosaki M, Matsuura K et al. (2009) Genome-wide association of IL28B with response to pegylated interferon-alpha and ribavirin therapy for chronic hepatitis C. Nat Genet 41: 1105-1109. doi:10.1038/ng.449. PubMed: 19749757.
38. Yoshizawa H (2002) Hepatocellular carcinoma associated with hepatitis C virus infection in Japan: projection to other countries in the foreseeable future. Oncology 62 Suppl 1: 8-17. doi:10.1159/000048270. PubMed: 11868791.
39. Sarasin-Filipowicz M, Oakeley EJ, Duong FH, Christen V, Terracciano L et al. (2008) Interferon signaling and treatment outcome in chronic hepatitis C. Proc Natl Acad Sci U S A 105: 7034-7039. doi:10.1073/pnas.0707882105. PubMed: 18467494.
40. Urban TJ, Thompson AJ, Bradrick SS, Fellay J, Schuppan D et al. (2010) IL28B genotype is associated with differential expression of intrahepatic interferon-stimulated genes in patients with chronic hepatitis C. Hepatology 52: 1888-1896. doi:10.1002/hep.23912. PubMed: 20931559.
41. Abe H, Hayes CN, Ochi H, Maekawa T, Tsuge M et al. (2011) IL28 variation affects expression of interferon stimulated genes and peg-interferon and ribavirin therapy. J Hepatol 54: 1094-1101. doi:10.1002/hep.24499. PubMed: 21145800.
42. Elyakim E, Sitbon E, Faerman A, Tabak S, Montia E et al. (2010) hsa-miR-191 is a candidate oncogene target for hepatocellular carcinoma therapy. Cancer Res 70: 8077-8087. doi:10.1158/0008-5472.CAN-10-1313. PubMed: 20924108.
43. Jangra RK, Yi M, Lemon SM (2010) miR-122 regulation of hepatitis C virus translation and infectious virus production. J Virol 84: 6615-6625. doi:10.1128/JVI.00417-10. PubMed: 20427538.
44. Fornari F, Gramantieri L, Giovannini C, Veronese A, Ferracin M et al. (2009) MiR-122/cyclin G1 interaction modulates p53 activity and affects doxorubicin sensitivity of human hepatocarcinoma cells. Cancer Res 69: 5761-5767. doi:10.1158/0008-5472.CAN-08-4797. PubMed: 19584283.
45. Tsai WC, Hsu SD, Hsu CS, Lai TC, Chen SJ et al. (2012) MicroRNA-122 plays a critical role in liver homeostasis and hepatocarcinogenesis. J Clin Invest 122: 2884-2897. doi:10.1172/JCI63455. PubMed: 22820290.
46. Hsu SH, Wang B, Kota J, Yu J, Costinean S et al. (2012) Essential metabolic, anti-inflammatory, and anti-tumorigenic functions of miR-122 in liver. J Clin Invest 122: 2871-2883. doi:10.1172/JCI63539. PubMed: 22820288.
47. Burns DM, D'Ambrogio A, Nottrott S, Richter JD (2011) CPEB and two poly(A) polymerases control miR-122 stability and p53 mRNA translation. Nature 473: 105-108. doi:10.1038/nature09908. PubMed: 21478871.

48. Lardizábal MN, Nocito AL, Daniele SM, Ornella LA, Palatnik JF et al. (2012) Reference genes for real-time PCR quantification of microRNAs and messenger RNAs in rat models of hepatotoxicity. PLOS ONE 7: e36323. doi:10.1371/journal.pone.0036323. PubMed: 22563491.
49. Norman KL, Sarnow P (2010) Modulation of hepatitis C virus RNA abundance and the isoprenoid biosynthesis pathway by microRNA miR-122 involves distinct mechanisms. J Virol 84: 666-670. doi: 10.1128/JVI.01156-09. PubMed: 19846523.
50. Li Y, Masaki T, Lemon SM (2013) miR-122 and the Hepatitis C RNA genome: More than just stability. RNA Biol 10: 919–24. PubMed: 23770926.
51. Janssen HL, Reesink HW, Lawitz EJ, Zeuzem S, Rodriguez-Torres M et al. (2013) Treatment of HCV Infection by Targeting MicroRNA. N Engl J Med, 368: 1685–94. PubMed: 23534542.
52. McGivern DR, Lemon SM (2011) Virus-specific mechanisms of carcinogenesis in hepatitis C virus associated liver cancer. Oncogene 30: 1969-1983. doi:10.1038/onc.2010.594. PubMed: 21258404.
53. Chen Y, Shen A, Rider PJ, Yu Y, Wu K et al. (2011) A liver-specific microRNA binds to a highly conserved RNA sequence of hepatitis B virus and negatively regulates viral gene expression and replication. FASEB J 25: 4511-4521. doi:10.1096/fj.11-187781. PubMed: 21903935.
54. Wang S, Qiu L, Yan X, Jin W, Wang Y et al. (2012) Loss of microRNA 122 expression in patients with hepatitis B enhances hepatitis B virus replication through cyclin G(1) -modulated P53 activity. Hepatology 55: 730-741. doi:10.1002/hep.24809. PubMed: 22105316.
55. Liu WH, Yeh SH, Chen PJ (2011) Role of microRNAs in hepatitis B virus replication and pathogenesis. Biochim Biophys Acta 1809: 678-685. doi:10.1016/j.bbagrm.2011.04.008. PubMed: 21565290.
56. Qiu L, Fan H, Jin W, Zhao B, Wang Y et al. (2010) miR-122-induced down-regulation of HO-1 negatively affects miR-122-mediated suppression of HBV. Biochem Biophys Res Commun 398: 771-777. doi:10.1016/j.bbrc.2010.07.021. PubMed: 20633528.
57. Liang Y, Shilagard T, Xiao SY, Snyder N, Lau D et al. (2009) Visualizing hepatitis C virus infections in human liver by two-photon microscopy. Gastroenterology 137: 1448-1458. doi:10.1053/j.gastro.2009.07.050. PubMed: 19632233.
58. Jung CJ, Iyengar S, Blahnik KR, Ajuha TP, Jiang JX et al. (2011) Epigenetic modulation of miR-122 facilitates human embryonic stem cell self-renewal and hepatocellular carcinoma proliferation. PLOS ONE 6: e27740. doi:10.1371/journal.pone.0027740. PubMed: 22140464.
59. Arai E, Ushijima S, Gotoh M, Ojima H, Kosuge T et al. (2009) Genome-wide DNA methylation profiles in liver tissue at the precancerous stage and in hepatocellular carcinoma. Int J Cancer 125: 2854-2862. doi: 10.1002/ijc.24708. PubMed: 19569176.
60. Jung JK, Park SH, Jang KL (2010) Hepatitis B virus X protein overcomes the growth-inhibitory potential of retinoic acid by downregulating retinoic acid receptor-beta2 expression via DNA methylation. J Gen Virol 91: 493-500. doi:10.1099/vir.0.015149-0. PubMed: 19828754.
61. Hsia CC, Thorgeirsson SS, Tabor E (1994) Expression of hepatitis B surface and core antigens and transforming growth factor-alpha in "oval cells" of the liver in patients with hepatocellular carcinoma. J Med Virol 43: 216-221. doi:10.1002/jmv.1890430304. PubMed: 7523580.
62. Pedersen IM, Cheng G, Wieland S, Volinia S, Croce CM et al. (2007) Interferon modulation of cellular microRNAs as an antiviral mechanism. Nature 449: 919-922. doi:10.1038/nature06205. PubMed: 17943132.
63. Wieland S, Thimme R, Purcell RH, Chisari FV (2004) Genomic analysis of the host response to hepatitis B virus infection. Proc Natl Acad Sci U S A 101: 6669-6674. doi:10.1073/pnas.0401771101. PubMed: 15100412.
64. Bigger CB, Guerra B, Brasky KM, Hubbard G, Beard MR et al. (2004) Intrahepatic gene expression during chronic hepatitis C virus infection in chimpanzees. J Virol 78: 13779-13792. doi:10.1128/JVI.78.24.13779-13792.2004. PubMed: 15564486.
65. Lanford RE, Guerra B, Bigger CB, Lee H, Chavez D et al. (2007) Lack of response to exogenous interferon-alpha in the liver of chimpanzees chronically infected with hepatitis C virus. Hepatology 46: 999-1008. doi:10.1002/hep.21776. PubMed: 17668868.

JVI
Journals.ASM.org

MicroRNA-27a Regulates Lipid Metabolism and Inhibits Hepatitis C Virus Replication in Human Hepatoma Cells

Takayoshi Shirasaki,[a,b] Masao Honda,[a,b] Tetsuro Shimakami,[a] Rika Horii,[a] Taro Yamashita,[a] Yoshio Sakai,[a] Akito Sakai,[a] Hikari Okada,[a] Risa Watanabe,[b] Seishi Murakami,[a] MinKyung Yi,[c] Stanley M. Lemon,[d] Shuichi Kaneko[a]

Department of Gastroenterology, Kanazawa University Graduate School of Medical Science, Kanazawa, Japan[a]; Department of Advanced Medical Technology, Kanazawa University Graduate School of Health Medicine, Kanazawa, Japan[b]; Human Center for Hepatitis Research, Institute for Human Infections and Immunity, and Department of Microbiology and Immunology, University of Texas Medical Branch, Galveston, Texas, USA[c]; Division of Infectious Diseases, School of Medicine, The University of North Carolina at Chapel Hill, Chapel Hill, North Carolina, USA[d]

The replication and infectivity of the lipotropic hepatitis C virus (HCV) are regulated by cellular lipid status. Among differentially expressed microRNAs (miRNAs), we found that miR-27a was preferentially expressed in HCV-infected liver over hepatitis B virus (HBV)-infected liver. Gene expression profiling of Huh-7.5 cells showed that miR-27a regulates lipid metabolism by targeting the lipid synthetic transcription factor RXRα and the lipid transporter ATP-binding cassette subfamily A member 1. In addition, miR-27a repressed the expression of many lipid metabolism-related genes, including *FASN*, *SREBP1*, *SREBP2*, *PPARα*, and *PPARγ*, as well as *ApoA1*, *ApoB100*, and *ApoE3*, which are essential for the production of infectious viral particles. miR-27a repression increased the cellular lipid content, decreased the buoyant density of HCV particles from 1.13 to 1.08 g/cm^3, and increased viral replication and infectivity. miR-27a overexpression substantially decreased viral infectivity. Furthermore, miR-27a enhanced *in vitro* interferon (IFN) signaling, and patients who expressed high levels of miR-27a in the liver showed a more favorable response to pegylated IFN and ribavirin combination therapy. Interestingly, the expression of miR-27a was upregulated by HCV infection and lipid overload through the adipocyte differentiation transcription factor C/EBPα. In turn, upregulated miR-27a repressed HCV infection and lipid storage in cells. Thus, this negative feedback mechanism might contribute to the maintenance of a low viral load and would be beneficial to the virus by allowing it to escape host immune surveillance and establish a persistent chronic HCV infection.

MicroRNA (miRNA) is a small, endogenous, single-stranded, noncoding RNA consisting of 20 to 25 bases that regulates gene expression. It plays an important role in various biological processes, including organ development, differentiation, and cellular death and proliferation, and is also involved in infection and diseases such as cancer (1).

Previously, we examined miRNA expression in hepatocellular carcinoma (HCC) and noncancerous background liver tissue infected with hepatitis B virus (HBV) and HCV (2). We showed that some miRNAs were differentially expressed according to HBV or HCV infection but not according to the presence of HCC. These infection-specific miRNAs were believed to regulate HBV or HCV replication; however, their functional role has not been elucidated.

HCV is described as a lipotropic virus because of its association with serum lipoprotein (3–5). It utilizes the low-density lipoprotein (LDL) receptor for cellular entry (6–8) and forms replication complexes on lipid rafts (9). The HCV core protein surrounds and binds lipid droplets (LDs) and nonstructural proteins on the endoplasmic reticulum (ER) membrane, which is essential for particle formation (10). Moreover, HCV cellular secretion is linked to very LDL (VLDL) secretion (11). In liver tissue histology, steatosis is often observed in chronic hepatitis C (CH-C) and is closely related to resistance to interferon (IFN) treatment (12, 13). Thus, lipids play important roles in HCV replication and CH-C pathogenesis.

Several miRNAs, such as miR-122 (14), miR-199a (15), miR-196 (16), miR-29 (17), Let-7b (18), and miR-130a (19), reportedly regulate HCV replication; however, miRNAs that regulate lipid metabolism and HCV replication have not been reported so far. Previously, we reported that 19 miRNAs were differentially expressed in HBV- and HCV-infected livers (2). In the present study, we evaluated the functional relevance of miR-27a in HCV replication by using the human hepatoma cell line Huh-7.5. We analyzed the regulation of lipid metabolism by miR-27a in hepatocytes and revealed a unique pathophysiological relationship between lipid metabolism and HCV replication in CH-C.

MATERIALS AND METHODS

Cell line. Huh-7.5 cells (kindly provided by C. M. Rice, Rockefeller University, New York, NY) were maintained in Dulbecco's modified Eagle's medium (DMEM; Gibco BRL, Gaithersburg, MD) containing 10% fetal bovine serum (FBS) and 1% penicillin-streptomycin.

HCV replication analysis. HCV replication analysis was performed by transfecting Huh-7.5 cells with JFH-1 (20), H77Sv2 Gluc2A (21), and their derivative RNA constructs. pH77Sv2 is a modification of pH77S, a plasmid containing the full-length sequence of the genotype 1a H77 HCV strain with five cell culture-adaptive mutations that promote its replication in Huh-7 hepatoma cells (21–24). pH77Sv2 Gluc2A is a related construct in which the *Gaussia* luciferase (Gluc) sequence, fused to the 2A autocatalytic protease of foot-and-mouth virus RNA, was inserted in frame between p7 and NS2 (21, 23, 25). pH77Sv2 Gluc2A (AAG) is a control plasmid that has an NS5B polymerase catalytic domain mutation.

Received 29 October 2012 Accepted 21 February 2013
Published ahead of print 28 February 2013
Address correspondence to Masao Honda, mhonda@m-kanazawa.jp.
Copyright © 2013, American Society for Microbiology. All Rights Reserved.
doi:10.1128/JVI.03022-12

For RNA transfection, the cells were washed with phosphate-buffered saline (PBS) and resuspended in complete growth medium. The cells were then pelleted by centrifugation (1,400 × *g* for 4 min at 4°C), washed twice with ice-cold PBS, and resuspended in ice-cold PBS at a concentration of 7.5×10^6 cells/0.4 ml. The cells were mixed with 10 μg of the RNA transcripts, placed into 2-mm-gap electroporation cuvettes (BTX Genetronics, San Diego, CA), and electroporated with five pulses of 99 μs at 750 V over 1.1 s in an ECM 830 (BTX Genetronics). Following a 10-min recovery period, the cells were mixed with complete growth medium and plated.

miR-27a and anti-miR-27a transfection. Huh-7.5 cells transfected with pH77Sv2 Gluc2A RNA or pH77Sv2 Gluc2A (AAG) RNA were transfected with 50 nM synthetic miRNA (pre-miRNA) or 50 nM anti-miRNA (Ambion Inc., Austin, TX) with the siPORTTM NeoFXTM Transfection Agent (Ambion). Transfection was performed immediately by mixing the electroporated cells with the miRNA transfection reagents. Control samples were transfected with an equal concentration of a nontargeting control (pre-miRNA negative control) or inhibitor negative control (anti-miRNA negative control) to assess non-sequence-specific effects in the miRNA experiments.

Fatty acid treatment. Huh-7.5 cells transfected with HCV RNA and pre- or anti-miRNA were cultured for 24 h and then treated with the indicated concentrations of oleic acid (0 to 250 μM) (26) in the presence of 2% free fatty acid (FFA)-free bovine serum albumin (BSA; Sigma-Aldrich, St. Louis, MO). The cells were harvested at 72 h posttreatment with oleic acid for quantitative real-time detection PCR (RTD-PCR), Western blotting, immunofluorescence staining, and reporter analysis. The number of viable cells was determined by an MTS assay [one-step 3-(4,5-dimethylthiazol-2-yl)-2,5-diphenyltetrazolium bromide assay; Promega Corporation, Madison, WI]. Cellular triglyceride (TG) and cholesterol (TCHO) contents were measured with TG Test Wako and Cholesterol Test Wako kits (Wako, Osaka, Japan) according to the manufacturer's instructions.

Equilibrium ultracentrifugation of JFH-1 particles in isopycnic iodixanol gradients. Filtered supernatant fluids collected from JFH-1 RNA- and pre-miRNA- or anti-miRNA-transfected cell cultures were concentrated 30-fold with a Centricon PBHK Centrifugal Plus-20 filter unit with an Ultracel PL membrane (100-kDa exclusion; Merck Millipore, Billerica, MA) and then layered on top of a preformed continuous 10 to 40% iodixanol (OptiPrep; Sigma-Aldrich) gradient in Hanks' balanced salt solution (Invitrogen, Carlsbad, CA) as described previously (24). The gradients were centrifuged in an SW41 rotor (Beckman Coulter Inc., Brea, CA) at 35,000 rpm for 16 h at 4°C, and the fractions (500 μl each) were collected from the top of the tube. The density of each fraction was determined with a digital refractometer (Atago, Tokyo, Japan).

Infectivity assays. Huh-7.5 cells were seeded at 5.0×10^4/well in 48-well plates 24 h before inoculation with 100 μl of the gradient fractions. The cells were tested for the presence of intracellular core antigen by immunofluorescence 72 h later, as described below. Clusters of infected cells that stained for the core antigen were considered to constitute a single infectious focus, and virus titers were calculated accordingly in terms of numbers of focus-forming units (FFU)/ml.

Western blotting and immunofluorescence staining. Western blotting was performed as described previously (27). The cells were washed in PBS and lysed in radioimmunoprecipitation assay buffer containing Complete protease inhibitor cocktail and PhosSTOP (Roche Applied Science, Indianapolis, IN). The membranes were blocked in Blocking One or Blocking One-P solution (Nacalai Tesque, Kyoto, Japan), and the expression of HCV core protein, retinoid X receptor alpha (RXRα), sterol regulatory element-binding protein (SREBP1), ATP-binding cassette subfamily A member 1 (ABCA1), ApoE3, ApoB100, fatty acid synthase (FASN), peroxisome proliferator-activated receptor α (PPARα), ApoA1, phospho-PKR-like ER kinase (phospho-PERK), PERK, phospho-eIF2α, eIF2α, BIP, phospho-STAT1, and β-actin was evaluated with mouse anti-core (Thermo Fisher Scientific Inc., Rockford, IL), rabbit anti-RXRα, rabbit anti-SREBP1 (Santa Cruz Biotechnology Inc., Santa Cruz, CA), mouse anti-ABCA1 (Abcam, Cambridge, MA), goat anti-ApoE3, goat anti-ApoB100 (R&D Systems Inc., Minneapolis, MN), rabbit anti-FASN, rabbit anti-PPARα, mouse anti-ApoA1, rabbit anti-phospho-PERK, rabbit anti-PERK, rabbit anti-phospho-eIF2α, rabbit anti-eIF2α, rabbit anti-BIP, rabbit anti-phospho-STAT1, and rabbit anti-β-actin antibodies (Cell Signaling Technology Inc., Danvers, MA), respectively.

For immunofluorescence staining, the cells were washed twice with PBS and fixed in 4% paraformaldehyde for 15 min at room temperature. After washing again with PBS, the cells were permeabilized with 0.05% Triton X-100 in PBS for 15 min at room temperature. They were then incubated in a blocking solution (10% FBS and 5% BSA in PBS) for 30 min and with the anti-core monoclonal antibodies. The fluorescent secondary antibodies were Alexa 568-conjugated anti-mouse IgG antibodies (Invitrogen). Nuclei were labeled with 4′,6-diamidino-2-phenylindole (DAPI), and LDs were visualized with boron-dipyrromethene (BODIPY) 493/503 (Invitrogen). Imaging was performed with a CSU-X1 confocal microscope (Yokogawa Electric Corporation, Tokyo, Japan).

Quantitative RTD-PCR. Total RNA was isolated with a GenElute Mammalian Total RNA Miniprep kit (Sigma-Aldrich), and cDNA was synthesized with a high-capacity cDNA reverse transcription kit (Applied Biosystems, Carlsbad, CA). The primer pairs and probes for C/EBPα, ABCA1, PPARγ, SREBF1, SREBF2, FASN, 2′-5′-oligoadenylate synthetase 2 (OAS2), and β-actin were obtained from the TaqMan assay reagent library. HCV RNA was detected as described previously (28). HCV RNA was isolated from viral particles with a QIAamp viral RNA kit (Qiagen, Inc., Valencia, CA) in accordance with the manufacturer's instructions. Total RNA containing miRNA was isolated according to the protocol of the mirVana miRNA isolation kit (Ambion). For the enrichment of mature miRNA, argonaute 2 (Ago2)-binding miRNA was immunoprecipitated with an anti-Ago2 monoclonal antibody (Wako) and mature miRNA was eluted from the precipitant with a microRNA isolation kit, Human Ago2 (Wako). cDNA was prepared via reverse transcription with 10 ng of isolated total RNA and 3 μl of each reverse transcription primer with specific loop structures. Reverse transcription was performed with a TaqMan MicroRNA reverse transcription kit (Applied Biosystems) according to the manufacturer's protocol. RTD-PCR was performed with the 7500 Real Time PCR system (Applied Biosystems) according to the manufacturer's instructions. The primer pairs and probes for miR-let7a, miR-34c, miR-142-5p, miR-27a, miR-23a, and RNU6B were obtained from the TaqMan assay reagent library.

3′ UTR luciferase reporter assays. The miRNA expression reporter vector pmirGLO Dual-Luciferase miRNA Target Expression Vector (Promega Corporation) was used to validate the RXRα and ABCA1 3′ untranslated regions (UTRs) as miRNA binding sites. cDNA fragments corresponding to the entire 3′ UTR of human RXRα and human ABCA1 were amplified with the Access RT-PCR system (Promega Corporation) from total RNA extracted from Huh-7.5 cells. The PCR products were cloned into the designated multiple cloning site downstream of the luciferase open reading frame between the SacI and XhoI restriction sites of the pCR2.1-TOPO vector (Invitrogen). Point mutations in the seed region of the predicted miR-27a sites within the 3′ UTR of human RXRα and human ABCA1 were generated with a QuikChange Multi site-directed mutagenesis kit (Agilent Technologies Inc., Santa Clara, CA) according to the manufacturer's protocol. All constructs were confirmed by sequencing.

Huh-7.5 cells were grown to 70% confluence in 24-well plates in complete DMEM. The cells were cotransfected with 200 ng of the indicated 3′ UTR luciferase reporter vector and 50 nM synthetic miRNA (pre-miRNA) or 50 nM anti-miRNA (Ambion) in a final volume of 0.5 ml with Lipofectamine 2000 (Invitrogen). At 24 h posttransfection, firefly and *Renilla* luciferase activities were measured consecutively with the Dual-Luciferase Reporter Assay system (Promega Corporation).

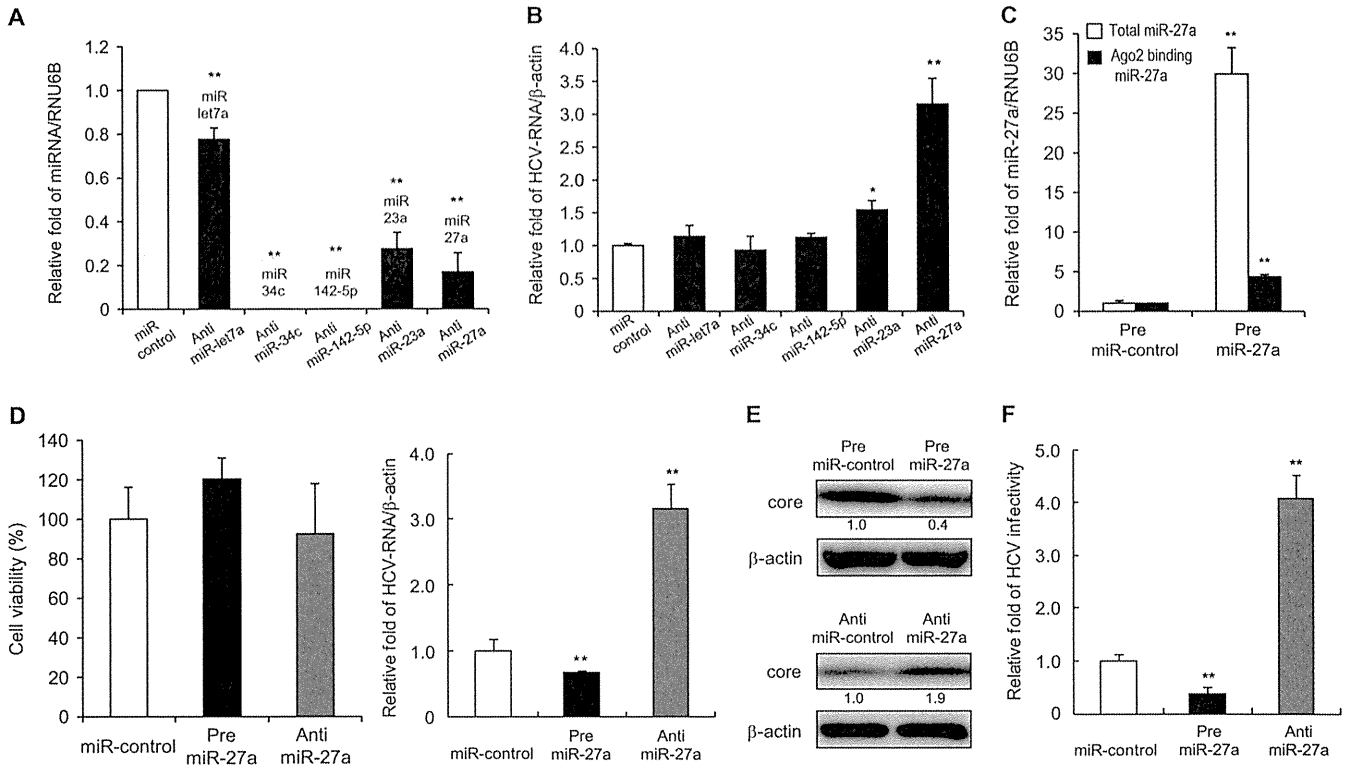

FIG 1 miR-27a has a negative effect on HCV replication and infectivity. Huh-7.5 cells were transfected with JFH-1 RNA and pre- or anti-miRNA. Expression was quantified at 72 h posttransfection. (A) Inhibition efficiency of miRNAs by anti-miRNAs (RTD-PCR, $n = 6$). (B) Effects of anti-miRNAs on HCV replication (RTD-PCR, $n = 6$). (C) Detection of whole miR-27a and Ago2-binding miR-27a in Huh-7.5 cells. At 72 h posttransfection, cells were harvested and Ago2-binding miRNA was purified as described in Materials and Methods. White bars indicate total miR-27a levels, and black bars indicate Ago2-binding miR-27a levels (RTD-PCR, $n = 6$). (D) Effects of pre- or anti-miR-27a on cell viability (left) and HCV replication (right). Cell viability (%) was assessed by the MTS assay ($n = 6$). (E) Effects of pre- or anti-miR-27a on HCV core protein levels by Western blotting. (F) Effects of pre- or anti-miR-27a on HCV infection. Huh-7.5 cells were infected with HCVcc derived from Huh-7.5 cells transfected with pre- or anti-miR-27a and JFH-1 RNA. HCV RNA was quantified at 72 h postinfection by RTD-PCR ($n = 6$). All experiments were performed in duplicate and repeated three times. Values are means ± standard errors. *, $P < 0.01$; **, $P < 0.005$.

Promoter analysis. DNA fragments from −400 to +36 bp and from −700 to +36 bp relative to the transcription initiation site of pri-miR-23a~27a~24-2 were inserted into pGL3-Basic (Promega Corporation) at the MluI and XhoI sites. Point mutations in the seed region of predicted C/EBPα binding sites were generated with a QuikChange Multi site-directed mutagenesis kit (Agilent Technologies) according to the manufacturer's protocol. All constructs were confirmed by sequencing.

Huh-7.5 cells transfected with HCV RNA were cultured for 24 h in 24-well plates, and then 200 ng of the plasmids was cotransfected with 2 ng of the *Renilla* luciferase expression vector (pSV40-Renilla) with the FuGENE6 Transfection Reagent (Roche Applied Science). After 24 h, the cells were treated with oleic acid in the presence of 2% FFA-free BSA (Sigma-Aldrich). At 48 h posttreatment, a luciferase assay was carried out with the Dual-Luciferase Reporter Assay system (Promega Corporation) according to the manufacturer's instructions.

For tunicamycin treatment, the plasmids (200 ng) were cotransfected with 2 ng pSV40-Renilla with FuGENE6 (Roche Applied Science) into Huh-7.5 cells grown in the wells of 24-well plates. After 24 h, the cells were treated for a further 24 h with the indicated concentrations of tunicamycin and a luciferase assay was carried out as described above.

RNA interference. A small interfering RNA (siRNA) specific to ABCA1 and a control siRNA were obtained from Thermo Fisher Scientific. Transfection was performed with Lipofectamine 2000 (Invitrogen) according to the manufacturer's instructions.

IFN treatment. Huh-7.5 cells transfected with HCV RNA and pre- or anti-miRNA were treated with oleic acid as described above. At 48 h later, the cells were treated with the indicated number of international units of IFN-α for 24 h.

Affymetrix GeneChip analysis. Aliquots of total RNA (50 ng) isolated from the cells were subjected to amplification with the WT-Ovation Pico RNA Amplification system (NuGen, San Carlos, CA) according to the manufacturer's instructions. The Affymetrix Human U133 Plus 2.0 microarray chip containing 54,675 probes has been described previously (29).

Statistical analysis. Results are expressed as mean values ± standard errors. At least six samples were tested in each assay. Significance was tested by one-way analysis of variance with Bonferroni methods, and differences were considered statistically significant at P values of <0.01 (*, $P < 0.01$; **, $P < 0.005$).

Microarray accession number. The expression data determined in this study were deposited in the Gene Expression Omnibus database (NCBI) under accession number GSE41737.

RESULTS

Functional relevance of the upregulated miRNAs in HCV-infected livers. Previously, 19 miRNAs were shown to be differentially expressed in HBV- and HCV-infected livers (2). Of these, 6 miRNAs were upregulated and 13 were downregulated. In this study, we focused on the upregulated miRNAs, as they might play a positive role in HCV replication. Anti-miRNAs and the control miRNA were transfected into Huh-7.5 cells following JFH-1 RNA

TABLE 1 Gene categories and names of differentially expressed genes regulated by miR-27a in Huh-7.5 cells

Protein function and name	Gene	Affy ID[a]	GB acc. no.[b]	Fold change		
				Pre-miR-27a/ miR-control	Anti-miR-27a/ anti-miR-control	Pre-miR-27a/ anti-miR-27a
Cytoskeleton remodeling and Wnt signaling						
Collagen, type IV, alpha 6	*COL4A6*	211473_s_at	U04845	0.85	2.19	2.58
Fibronectin 1	*FN1*	214702_at	AJ276395	0.57	1.14	2.02
Filamin A, alpha	*FLNA*	214752_x_at	AI625550	0.64	1.68	2.61
LIM domain kinase 1	*LIMK1*	204357_s_at	NM_002314	0.67	1.63	2.43
p21/Cdc42/Rac1-activated kinase 1	*PAK1*	230100_x_at	AU147145	0.63	1.58	2.53
Breast cancer anti-estrogen resistance 1	*BCAR1*	232442_at	AU147442	0.96	1.94	2.01
Frizzled homolog 3 (*Drosophila*)	*FZD3*	219683_at	NM_017412	0.51	1.30	2.55
Laminin, alpha 4	*LAMA4*	210990_s_at	U77706	0.63	1.26	2.00
Regulation of lipid metabolism						
CREB binding protein (Rubinstein-Taybi syndrome)	*CREBBP*	235858_at	BF507909	0.54	1.50	2.76
NF-Y	*NF-Y*	228431_at	AL137443	0.41	1.44	3.50
Sterol regulatory element binding transcription factor 2	*SREBF2*	242748_at	AA112403	0.47	1.11	2.35
Membrane-bound transcription factor peptidase, site 2	*MBTPS2*	1554604_at	BC036465	0.50	1.21	2.39
Adenosine A2A receptor signaling						
Mitogen-activated protein kinase kinase 7	*MAP2K7*	226053_at	AI090153	0.90	2.07	2.31
Par-6 partitioning defective 6 homolog beta	*PARD6B*	235165_at	AW151704	0.56	1.35	2.43
Rap guanine nucleotide exchange factor (GEF) 2	*RAPGEF2*	238176_at	T86196	0.46	1.36	2.98
Ribosomal protein S6 kinase, 90kDa, polypeptide 2	*RPS6KA2*	204906_at	BC002363	0.61	1.72	2.83
p53 regulation						
MDM2	*MDM2*	237891_at	AI274906	0.41	1.27	3.07
Ubiquitin B	*UBB*	217144_at	X04801	0.58	1.89	3.24
Promyelocytic leukemia	*PML*	235508_at	AW291023	0.52	1.45	2.80
SMT3 suppressor of mif two 3 homolog 1	*SUMO1*	208762_at	U83117	0.55	1.23	2.22
IL-8 in angiogenesis						
B-cell CLL/lymphoma 10	*BCL10*	1557257_at	AA994334	0.59	1.23	2.08
Janus kinase 2	*JAK2*	205841_at	NM_004972	0.77	1.71	2.23
Sphingosine-1-phosphate receptor 1						
G protein, alpha inhibiting activity polypeptide 2	*GNAI2*	201040_at	NM_002070	0.69	1.49	2.15
G protein, beta polypeptide 4	*GNB4*	223487_x_at	AW504458	0.86	1.78	2.06
Mitogen-activated protein kinase 1	*MAPK1*	1552263_at	NM_138957	0.87	1.93	2.22
GRB2-associated binding protein 1	*GAB1*	226002_at	AK022142	0.66	1.40	2.11

[a] Affy ID, Affymetrix identification number.
[b] GB acc. no., GenBank accession number.

transfection. The efficiency with which these anti-miRNAs inhibit the miRNAs is shown in Fig. 1A. Unexpectedly, inhibition of these miRNAs either had no effect or increased HCV replication in the cases of anti-miR-23a and anti-miR-27a (Fig. 1B).

To investigate the functional relevance of miR-27a in HCV replication in more detail, we evaluated JFH-1 replication in Huh-7.5 cells in which miR-27a was inhibited or overexpressed. The efficacy of miR-27a overexpression is shown in Fig. 1C. Although ectopically introduced pre-miR-27a increased miR-27a levels by approximately 30-fold, the levels of endogenous active Ago2 bound to miR-27a in RNA-induced silencing complexes increased by approximately 5-fold. The RNA and core protein levels of JFH-1 in Huh-7.5 cells decreased to 65% and 40%, respectively, following miR-27a overexpression. In contrast, the RNA and core protein levels of JFH-1 increased by 3- and 1.9-fold, respectively, following miR-27a inhibition (Fig. 1D and E). There was no significant difference in cell viability following miR-27a overexpression or inhibition (Fig. 1D). Furthermore, the rate of Huh-7.5 cell infection by JFH-1 decreased to 35% after the overexpression of miR-27a but increased 4-fold after miR-27a inhibition (Fig. 1F). Thus, miR-27a negatively regulates HCV replication and infection.

miR-27a targets the signaling pathways of cytoskeleton remodeling and lipid metabolism in Huh-7.5 cells. We next examined which signaling pathways were modulated by miR-27a. TargetScan (http://www.targetscan.org/) predicts biological targets of miRNAs by searching for the presence of conserved 8- and 7-mer sites that match the seed region of each miRNA (30). A TargetScan (release 5.2) for miR-27a predicted 921 candidate target genes, and functional gene ontology enrichment analysis of these genes by MetaCore (Thomson Reuters, New York, NY) showed that miR-27a could target the cytoskeleton remodeling and lipid metabolism signaling pathways (data not shown).

To examine whether these signaling pathways were regulated by miR-27a, gene expression profiling was carried out with Huh-7.5 cells in which miR-27a was over- or underexpressed. Transfection of cells with pre-miR-27a and pre-miR-

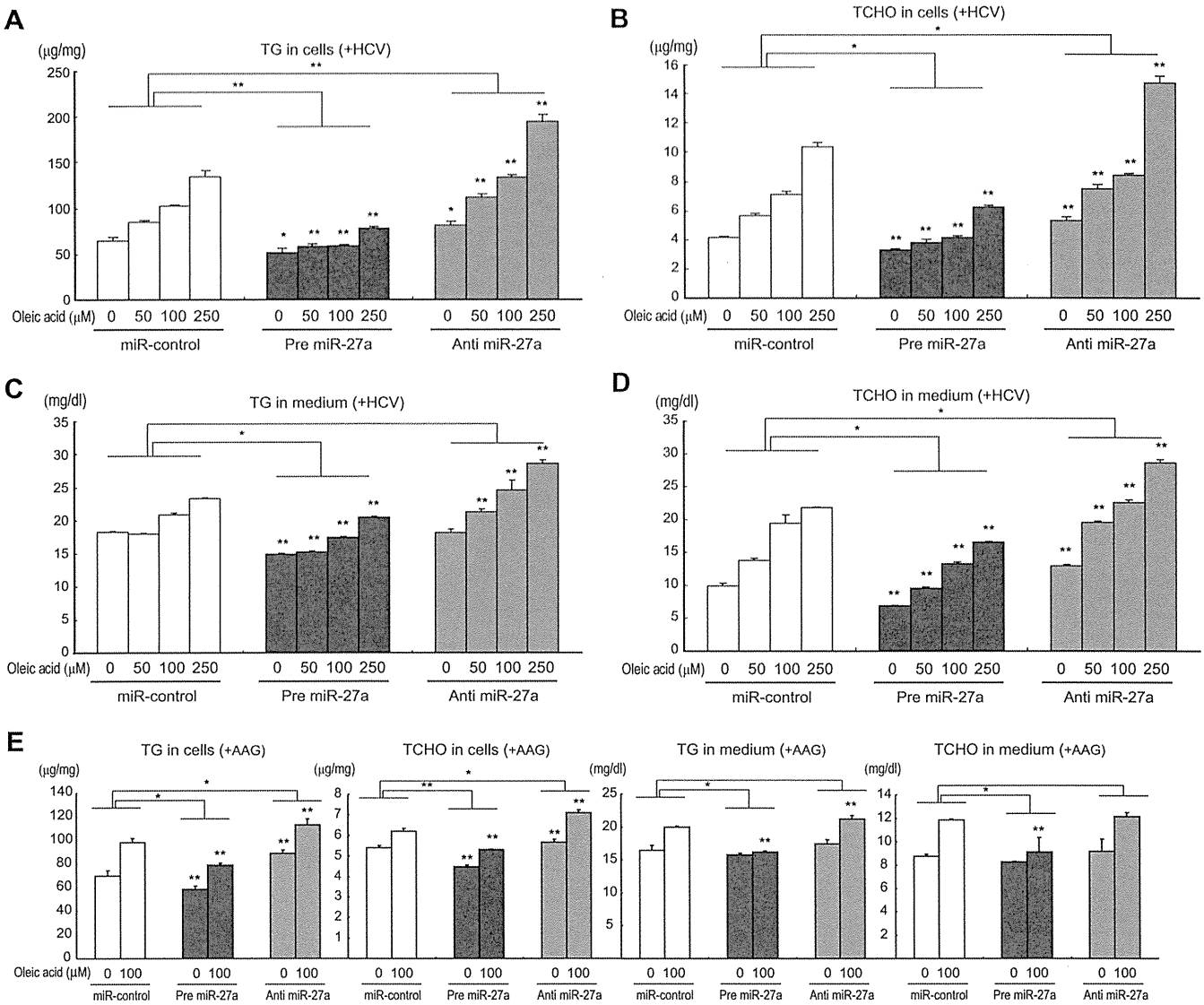

FIG 2 Changes in the lipid contents of Huh-7.5 cells and culture medium caused by pre- and anti-miR-27a. Huh-7.5 cells were transfected with replication-competent HCV RNA (H77Sv2 Gluc2A RNA [+HCV]) or replication-incompetent HCV RNA [H77Sv2 Gluc2A (AAG) (+AAG)] together with pre- or anti-miR-27a. At 24 h posttransfection, increasing amounts of oleic acid (0 to 250 μM) were added to the culture medium, and at 72 h after oleic acid treatment, TG and TCHO levels were measured in the cells and medium. Panels: A, TG in cells; B, TCHO in cells; C, TG in medium; D, TCHO in medium; E, TG and TCHO in cells and medium; A to D, +H77Sv2 Gluc2A (+HCV); E, +H77Sv2 Gluc2A (AAG) (+AAG). Lipid concentration was compared with that of miR-control and pre- or anti-miRNA ($n = 6$). All experiments were performed in duplicate and repeated three times. Values are means ± standard errors. *, $P < 0.01$; **, $P < 0.005$.

control or with anti-miR-27a and anti-miR-control enabled the identification of down- and upregulated genes, respectively. A total of 870 genes were selected with a >2-fold anti-miR-27a/pre-miR-27a expression ratio. Pathway analysis of these genes with MetaCore revealed that they are involved in cytoskeleton remodeling signaling, including that of *COL4A6*, *FN 1*, and *PAK1*; lipid metabolism signaling, including that of *CREBBP* and *SREBF2*; A2A receptor signaling, including that of *RAPGEF2*; and p53 regulation signaling, including that of *MDM2*. These genes were repressed by miR-27a in Huh-7.5 cells (Table 1).

miR-27a reduces TG and TCHO levels in cells and culture medium. Pathway analysis of the gene expression profile regulated by miR-27a in Huh-7.5 cells revealed the presence of many genes involved in lipid metabolism-related signaling pathways. To examine the functional relevance of miR-27a in lipid metabolism, we measured the cellular levels of TG and TCHO in Huh-7.5 cells in which miR-27a was inhibited or overexpressed, respectively. As shown in Fig. 2A and B, TG and TCHO levels in Huh-7.5 cells transfected with miR-control were increased in a dose-dependent manner following the addition of oleic acid (0 to 250 μM). Pre-miR-27a repressed this increase, while anti-miR-27a significantly accelerated it. Similarly, pre-miR-27a repressed the increase in TG and TCHO in the culture medium, while anti-miR-27a significantly accelerated it (Fig. 2C and D).

Similar results were obtained with both HCV-replicating cells

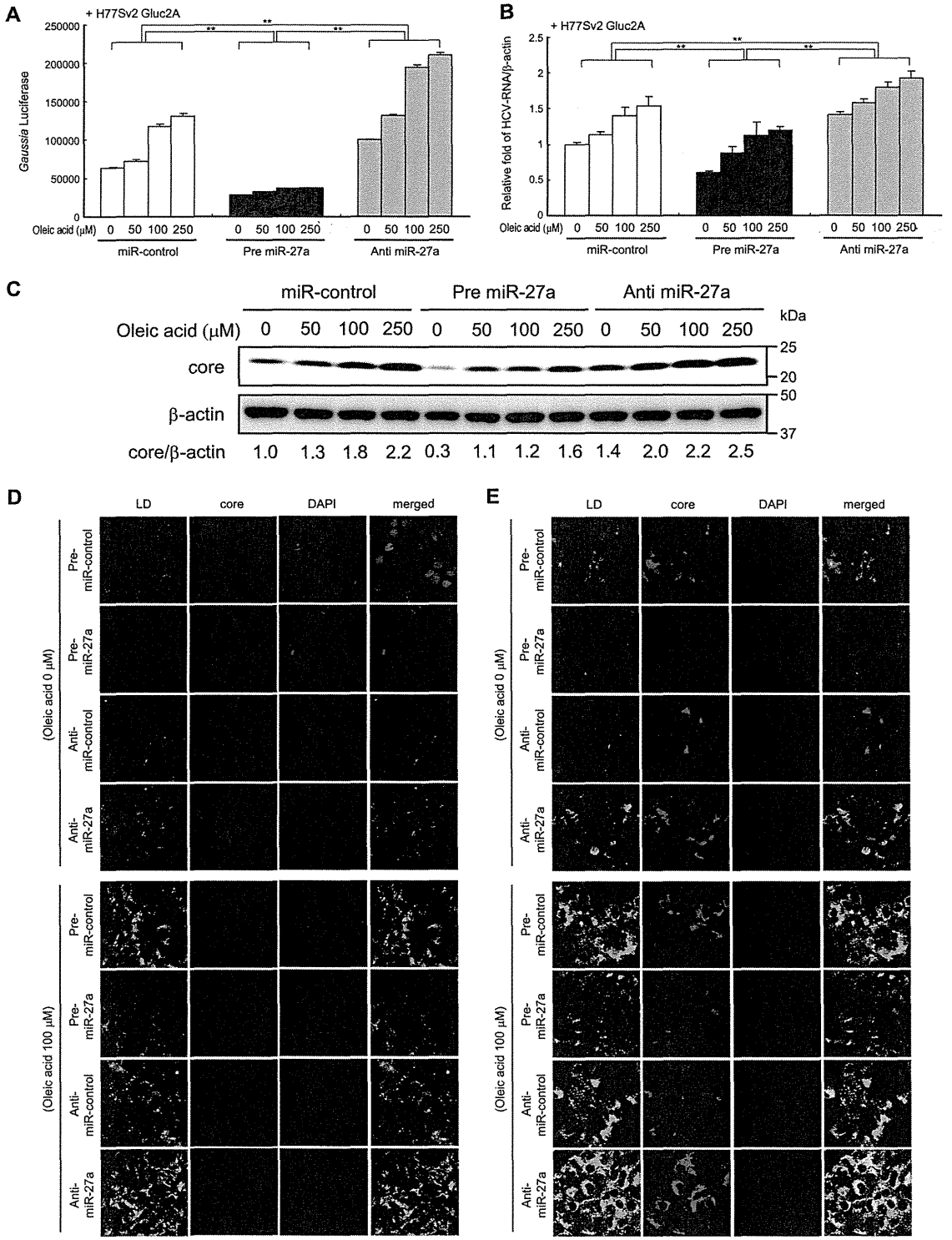

FIG 3 Changes in HCV replication in Huh-7.5 cells caused by pre- and anti-miR-27. Huh-7.5 cells were transfected with H77Sv2 Gluc2A RNA or H77Sv2 Gluc2A (AAG) RNA and pre- or anti-miR-27a. At 24 h posttransfection, increasing amounts of oleic acid (0 to 250 μM) were added to the culture medium. At 72 h after oleic acid treatment, the cells were harvested. (A) Gluc activity in the medium reflecting HCV replication in cells ($n = 6$). (B) Effects of pre- or anti-miR-27 on HCV RNA levels (RTD-PCR, $n = 6$). Experiments were performed in duplicate and repeated three times. Values are means ± standard errors. *, $P < 0.01$; **, $P < 0.005$. (C) Western blotting of HCV core protein in the same experiments. (D and E) Confocal microscopy images of Huh-7.5 cells in the same experiments. D, +H77Sv2 Gluc2A (AAG); E, +H77Sv2 Gluc2A. Cells were fixed, permeabilized, and stained with an anti-HCV core protein antibody. Nuclei were labeled with DAPI. LDs were visualized with BODIPY 493/503 dye. Imaging was performed with a CSU-X1 confocal microscope.

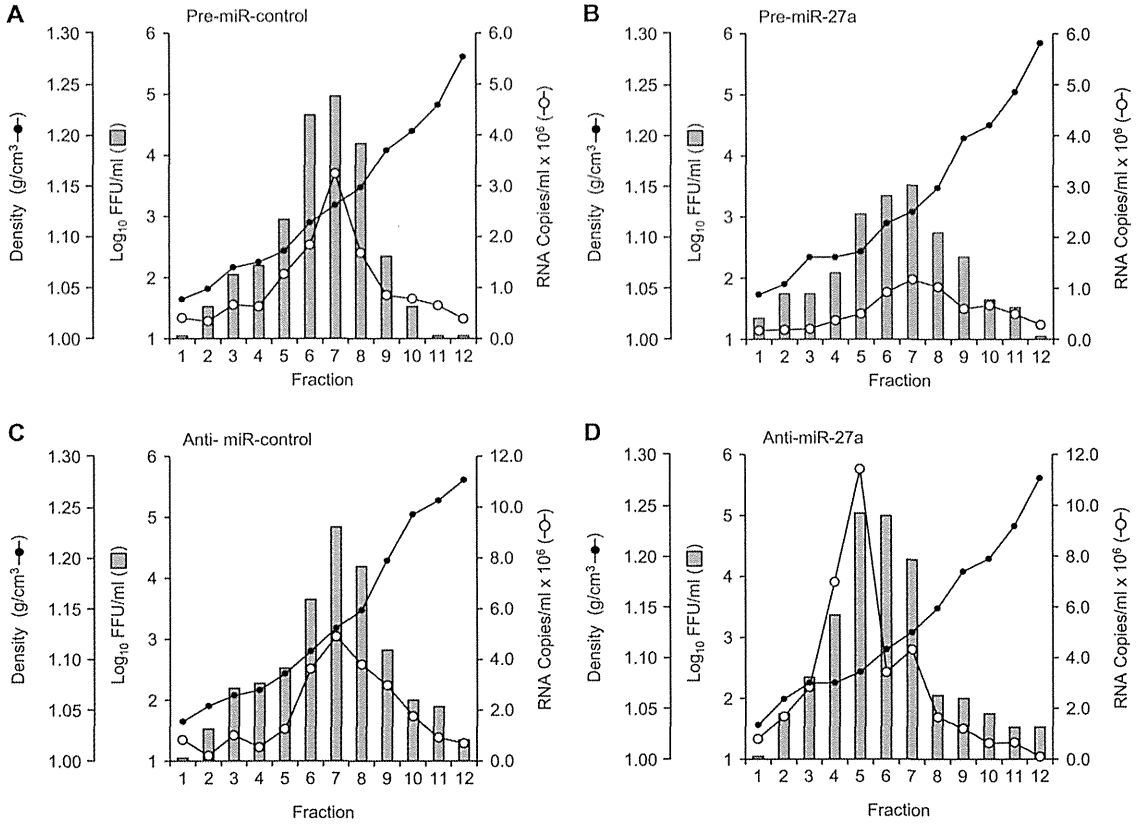

FIG 4 Equilibrium ultracentrifugation of JFH-1 particles in isopycnic iodixanol gradients. Filtered supernatant fluids collected from JFH-1 RNA- and pre- or anti-miRNA-transfected Huh-7.5 cell cultures were concentrated and used to collect fractions (500 μl each). Black circles indicate the gradient densities of the fractions, white circles indicate the HCV RNA titers, and bars indicate HCV infectivity levels. Panels: A, cells overexpressing pre-miR-control; B, cells overexpressing pre-miR-27a; C, cells overexpressing anti-miR-control; D, cells overexpressing anti-miR-27a. Experiments were repeated twice.

(+HCV) (Fig. 2A to D) and non-HCV-replicating cells (+AAG) (Fig. 2E), although the changes in the levels of TG and TCHO in the culture medium were smaller for the non-HCV-replicating cells (+AAG) (Fig. 2E). Correlating with the lipid component findings, replication of the infectious HCV clone H77Sv2 Gluc2A (21), as determined by Gluc activity in the culture medium, and the HCV RNA titer were significantly repressed by pre-miR-27a and increased by anti-miR-27a (Fig. 3A and B). This result was also confirmed by the core protein levels determined by Western blotting (Fig. 3C).

The localization of LDs and core proteins in the cells was visualized by confocal laser microscopy with a lipotropic fluorescent dye and immunostaining of the core protein (Fig. 3E). The LD and core protein levels were substantially repressed by pre-miR-27a and greatly increased by anti-miR-27a antibody. The change in the levels of LDs caused by miR-27a was observed in both HCV-replicating cells (Fig. 3E) and non-HCV-replicating cells (Fig. 3D), although the magnitude of the change was more prominent in HCV-replicating cells.

miR-27a changes the buoyant density and infectivity of HCV particles. The culture medium of Huh-7.5 cells in which JFH-1 was replicating was fractionated by iodixanol gradient centrifugation, and the buoyant density of HCV particles was evaluated (Fig. 4). When the cells were transfected with control miRNA (pre-miR-control and anti-miR-control), the HCV RNA titer (number of copies/ml) and infectivity (number of FFU/ml) peaked at fraction 7 (Fig. 4A and D) and the buoyant density of HCV was estimated at around 1.13 g/cm^3. Transfection with pre-miR-27a did not change the buoyant density of HCV, but it reduced the HCV RNA titer to 0.25-fold of the control and HCV infectivity to 0.024-fold of the control (Fig. 4B). In contrast, transfection with anti-miR-27a reduced the buoyant density of HCV from 1.13 to 1.08 g/cm^3 (Fig. 4B) and increased the HCV RNA titer to 2.1-fold of the control and infectivity to 2.5-fold of the control (Fig. 4C and D). Thus, miR-27a changed the buoyant density and infectivity of HCV.

miR-27a regulates lipid metabolism-related gene expression. The regulation of lipid metabolism-related genes by miR-27a was evaluated in Huh-7.5 cells (Fig. 5 and 6). The lipid synthesis transcription factors PPARγ, FASN, SREBP1, SREBP2, and RXRα were slightly, but significantly, induced in cells in which H77Sv2 Gluc2A replicated. The expression of lipid synthesis transcription factors was compared with that from cells carrying replication-incompetent H77Sv2 Gluc2A (AAG) (Fig. 5 and 6). Unexpectedly, lipid overload with oleic acid had no effect or rather decreased the levels of these transcription factors in non-HCV-replicating cells, probably because of negative feedback mechanisms. Conversely, in HCV-replicating cells, lipid overload with oleic acid further increased the levels of these transcription factors at both the